NASA Technical Memorandum 86425

Preliminary Design Study of a Lateral-Directional Control System Using Thrust Vectoring

Frederick J. Lallman

NOVEMBER 1985

NASA Technical Memorandum 86425

Preliminary Design Study of a Lateral-Directional Control System Using Thrust Vectoring

Frederick J. Lallman
Langley Research Center
Hampton, Virginia

NASA
National Aeronautics
and Space Administration

Scientific and Technical Information Branch

1985

Summary

Thrust-vectoring engine nozzles raise new possibilities for controlling future generations of jet airplanes Aerodynamic control surfaces are conventionally used to generate the moments required to pitch, roll, and yaw airplanes. These moments become weak during low-speed flight because of low dynamic pressure. At high angles of attack, aerodynamic controls are corrupted by cross-axis coupling terms, which complicate the design of control systems Thrust-vectoring controls, on the other hand, are especially effective when the dynamic pressure is relatively low. The moments generated by thrust-vectoring controls remain aligned with the axes of the airplane regardless of the angle of attack. The incorporation of thrust-vectoring controls into jet airplane designs promises to extend the low-speed region of the flight envelope and may influence in-flight maneuver capabilities and airfield operations In addition, thrust-vectoring controls provide redundancy for the aerodynamic controls, which is a significant advantage in the event of failures or damage. This report documents a study undertaken to explore the application of thrust-vectoring controls to the lateral and directional control of a jet fighter airplane. The result of the study is a preliminary feedback control system design for a specific airplane configuration.

A mathematical model representative of a modern high-performance twin-jet fighter airplane including ailerons, rudder, and independent horizontal-tail surfaces was formulated Idealized bidirectional thrust-vectoring nozzles capable of generating control moments about the three airplane axes were added to this model. Linear perturbation equations for level, trimmed flight were calculated for angles of attack ranging from 0° to 90°. Scheduled gains between the control effectors and two pseudo control variables were found. These schedules were selected so that changes in a lateral pseudo control variable would cause coordinated aerodynamic and thrust-vectoring control motions which would influence the roll and spiral modes of the airplane with little disturbance of the Dutch roll mode In a similar fashion, a directional pseudo control variable was chosen such that it would mainly influence the Dutch roll mode. A modified system of perturbation equations was formed by combining these schedules with the original perturbation equations. The inputs of the modified system were the two pseudo control variables. Feedback and feedforward gains were obtained by solving a linear quadratic regulator problem using quadratic penalties on the differences between the airplane responses to lateral stick and rudder pedal movements and idealized responses. These gains were then scheduled as functions of angle of attack.

Simulated responses to step pilot control inputs were stable and well behaved. For lateral stick deflections, peak stability axis roll rates were between 1 25 and 1.60 rad/sec over a range of angle of attack of 10° to 70°. For rudder pedal deflections, the roll rates accompanying the sideslip responses could be arrested by small lateral stick motions.

Introduction

Lateral control and directional control of airplanes are traditionally treated as separate design problems. Rolling maneuvers (lateral control) are performed by lateral deflections of the control stick, which activate the ailerons to produce rolling moments Sideslipping maneuvers (directional control) are performed by deflections of the rudder pedals, which activate the rudder to produce yawing moments Acceptable control of most airplanes is achieved by mechanical systems which move the control surfaces in proportion to the cockpit controls and by designing the airplane so that it is aerodynamically stable and well behaved.

Modern high-performance airplanes which have wide flight envelopes are often difficult to handle with traditional control strategies in certain flight regimes Electronic systems are used in these airplanes to produce artificial stability and improve handling qualities. Stability augmentation systems improve the damping of airplane motions, cause the airplane to respond better to the pilot's control motions, make the expansion of flight envelopes possible, and permit innovations in airframe design. As these systems have evolved, they have remained segregated into lateral and directional systems even though there may be crossfeeds between them, for example, the aileron-rudder-interconnect used during flight at high angles of attack.

Additional complications arise when new types of control effectors are added to yield unconventional airplane configurations. The ailerons may be augmented by spoilers and differential deflections of the horizontal tail, for example, and the rudder may be augmented by lateral thrust vectoring. Different control effectors are effective during different flight phases. For example, aerodynamic control surfaces can easily overpower thrust-vectored controls during high-speed flight but become inferior at low speeds.

Controls which are effective for a given mode at one flight condition may affect a different mode at another flight condition. For example, the ailerons, which excite the roll mode during cruising flight, can cause directional oscillations during flight at high angles of attack because of excitation of the

Dutch roll mode. Scheduling of the control devices is necessary to maintain desired airplane response to the pilot inputs throughout the flight envelope. The design of stability augmentation systems by the traditional axis-by-axis approach is becoming increasingly complicated because of (1) the widening range of flight conditions in which new airplanes must operate and (2) the large selection of control effectors available for new airframe designs.

Modern multivariable controls methodology makes the simultaneous design of lateral and directional controls possible. The stability and control characteristics of both axes are improved, and multiple redundant controls are utilized in the most advantageous manner. Translation of the results of multivariable techniques into practical control system implementations is cumbersome The solutions are in the form of a matrix of gains, one gain for each state variable–control variable combination. Implementation requires the measurement or estimation of all the state variables. Each gain may be expected to vary with changing flight condition. There is no distinction between lateral and directional control systems. Such a distinction is desirable because it permits analysis of system elements which can be related to recognizable items present in conventional control systems

A preliminary design of a lateral-directional control system for a fighter airplane utilizing thrust-vectoring engine nozzles is presented in this report. The incorporation of thrust-vectoring controls into jet airplane designs promises to extend the low-speed region of the flight envelope and may influence in-flight maneuver capabilities and airfield operations. The control system is specified for a wide angle-of-attack range, and the airplane has several redundant moment generators. This redundancy is a significant advantage in the event of failures or damage Such design problems are representative of the types that are currently challenging airplane designers.

The present study maintains the distinction between the lateral and directional control systems while utilizing multivariable design techniques to specify the system gains The control effectors are scheduled to form lateral and directional control channels by the application of the relative controls effectiveness technique of reference 1. Gains which specify the lateral and directional feedback signals are obtained by the solution of a linear quadratic regulator (LQR) problem. Signals from onboard sensors are combined to form the feedback signals The feedback gains are scheduled for operation over a wide range of flight conditions. Comparisons and relative evaluations of the control system are beyond the scope of this report.

Symbols

$\mathbf{A}$	matrix of state variable coefficients
a_y	measured lateral acceleration, m/sec^2
$a_{y,cg}$	lateral acceleration of center of gravity, m/sec^2
$\mathbf{B}$	matrix of control variable coefficients
b	wing span, m
$\mathbf{C}$	control-mixing matrix
C_D	aerodynamic drag coefficient
C_{eff}	relative control effectiveness measure (see ref. 1)
C_L	aerodynamic lift coefficient
C_l	aerodynamic rolling-moment coefficient
C_m	aerodynamic pitching-moment coefficient
C_n	aerodynamic yawing-moment coefficient
C_Y	aerodynamic side-force coefficient
CCV	control configured vehicle
$\bar{c}$	mean aerodynamic chord, m
D	drag force, N
$\mathbf{F}$	state variable feedback matrix
$\mathbf{F}_b$	measurement variable feedback matrix
$\vec{f}$	vector of coefficients relating state variables to lateral acceleration
$\mathbf{G}$	matrix of pseudo control influences upon measurement vector
g	gravitational constant, 9.81 m/sec^2
$\vec{g}$	vector of coefficients relating control variables to lateral acceleration
$\mathbf{H}$	matrix of state variable influences upon measurement vector
$\mathbf{I}$	identity matrix
I_{xz}	product of inertia, kg-m^2
I_z	moment of inertia, kg-m^2
J	performance index
L	lift force, N

LQR	linear quadratic regulator
l_{cp}	distance of center of percussion from center of gravity, m
l_t	distance of tail from center of gravity, m
M	pitching moment, N-m
m	mass, kg
p	body axis roll rate, rad/sec
p_m	stability axis roll rate model, rad/sec
p_s	stability axis roll rate, rad/sec
q	pitch rate, rad/sec
$\bar{q}$	dynamic pressure, Pa
r	body axis yaw rate, rad/sec
r_m	stability axis yaw rate model, rad/sec
S	reference wing area, m^2
s	Laplace transform variable, sec^{-1}
T	thrust, N
T_{ce}	turn coordination error, rad/sec
t	time, sec
$\mathbf{u}$	vector of control variables (denoted by $\vec{u}$ on fig. 19)
V	true airspeed, m/sec
V_1	= max(50,V), m/sec
$\mathbf{v}$	vector of pseudo control variables
v_{dir}	directional pseudo control variable
v_{lat}	lateral pseudo control variable
W	weight, N
$\mathbf{x}$	vector of state variables (denoted by $\vec{x}$ on fig. 19)
$\mathbf{y}_m$	vector of measurements
y_1	difference between stability axis roll rate and roll rate model, rad/sec
y_2	difference between actual and desired turn coordination error, rad/sec
y_3	integrated error of lateral acceleration, m/sec
α	angle of attack, deg
β	angle of sideslip, deg
β_{est}	estimated angle of sideslip, rad
$\dot{\beta}_{est}$	estimated rate of change of angle of sideslip, rad/sec
γ	flight path angle, deg
δ_a	aileron deflection, deg (positive, right aileron up)
δ_D	differential horizontal-tail deflection, deg (positive, right trailing edge up)
δ_h	horizontal-tail deflection, deg (positive, trailing edge down)
δ_r	rudder deflection, deg (positive, trailing edge left)
δ_{rp}	rudder pedal deflection, portion of full deflection (positive, left pedal depressed)
δ_s	control stick lateral deflection, portion of full deflection (positive for deflection to right)
$\delta_{v,pitch}$	pitching thrust vector, deg (positive, nozzles down)
$\delta_{v,roll}$	rolling thrust vector, deg (positive, right nozzle up)
$\delta_{v,yaw}$	yawing thrust vector, deg (positive, nozzles left)
η_1, η_2	Gaussian white noise variables
θ	pitch angle, deg
λ	eigenvalue, sec^{-1}
ξ	damping ratio
ρ	air density, kg/m^3
ϕ	bank angle, deg
ω_n	natural frequency, rad/sec

A dot ($\cdot$) over a variable denotes differentiation with respect to time. Derivatives of aerodynamic coefficients with respect to angle of attack, sideslip angle, or any of the control deflections are denoted by subscripts as, for example, $C_{L_\alpha} = \partial C_L / \partial \alpha$. Derivatives of aerodynamic coefficients with respect to pitch rate are scaled by $\bar{c}/2V$ as, for example, $C_{m_q} = (2V/\bar{c})\ \partial C_m / \partial q$. Derivatives of aerodynamic coefficients with respect to roll rate and yaw rate are scaled by $b/2V$ as, for example, $C_{l_p} = (2V/b)\ \partial C_l / \partial p$. The measure of filter gain (in decibels, dB) is calculated as 20 times the common logarithm of the gain.

Design Procedure Outline

The steps used in the design procedure of developing the lateral-directional control system for the fighter airplane utilizing thrust-vectoring engine nozzles are briefly outlined in this section. More exhaustive elaboration is presented in following sections. The steps of the design procedure are

1. Construct a mathematical dynamic model
2. Find a set of trim conditions and perturbation equations.
3. Form pseudo control variables.
4. Solve a linear quadratic regulator problem
5. Modify the feedback variable set.
6 Delete ineffective gain elements.
7. Schedule the gains.

The unique feature of this process is the third step, in which five control effector variables are transformed into two pseudo control variables This step reduces the dimension of the gain matrix which must be processed in the remaining steps.

The first step of the design procedure is to construct a mathematical model of the airplane dynamics. The aerodynamic coefficients used are simplified functions of angle of attack. Generally, these were constructed of piecewise linear and low-order-polynomial segments selected to reasonably fit the available wind-tunnel data and to provide continuous derivatives where needed The aerodynamic coefficients were defined for an angle-of-attack range of 0° to 90°.

Idealized bidirectional thrust-vectoring engine nozzles were appended to the airplane mathematical model to provide additional control moments. Pitching moments were generated by simultaneously vectoring the engine nozzles in the pitch plane of the airplane. Yawing moments were generated by simultaneously vectoring the nozzles laterally. Rolling moments were generated by differentially vectoring the nozzles in the pitch plane. This thrust-vectoring capability permits controlled flight at high angles of attack and low airspeeds, at which the aerodynamic controls are ineffective

The mathematical model was trimmed for horizontal flight at constant airspeed for angles of attack up to 90° (hovering flight). The horizontal tail was used to provide the necessary pitching moment until it reached its maximum deflection near the stall angle of attack At higher angles of attack, the thrust of the engines was vectored in the airplane pitch plane to supplement the horizontal tail. The dynamics of perturbations about these trim conditions were found These linear perturbation dynamics were used in the development of the control system

The next step was to determine schedules for the five lateral-directional controls (ailerons, rudder, differential horizontal tail, and rolling-moment-producing and yawing-moment-producing thrust vectors). To accomplish this, the relative control effectiveness technique of reference 1 was applied to the perturbation equations. Two "pseudo" control variables were found, with one concentrating its effectiveness on the roll and spiral modes and with the other primarily affecting the Dutch roll mode. Activation of each of the pseudo control variables resulted in proportional deflections of the lateral-directional controls. The calculated ratios of the control deflections to the pseudo control variables changed with flight condition These ratios were used as the basis for constructing schedules to interconnect the lateral-directional controls. Because of the uncertainty of having reliable air-data information available near or beyond stall, the schedules were frozen during flight in these regimes. The control schedules were combined with the linear perturbation models to form modified perturbation models whose inputs were the pseudo control variables The use of the pseudo controls minimized coupling of the modes of the airplane and reduced the number of control variables in the subsequent steps of the design procedure

A linear quadratic regulator (LQR) problem was formulated to obtain feedback and feedforward gains which augmented the stability of the airplane and specified the signal paths from the cockpit controllers (stick and rudder pedals) and the state variables to the pseudo control variables. The modified perturbation equations were augmented by lateral and directional pilot models. In each case the pilot was modelled by a Gaussian random variable driving a first-order lag. Two such first-order lags were included to provide idealized airplane lateral and directional responses to the pilot model commands. The integral of the lateral acceleration was included to minimize long-term errors in turn coordination. The quadratic performance index for the LQR problem included weights on the differences between the airplane responses and the idealized responses, the integral of the lateral acceleration, and the pseudo control variables.

The gain matrix resulting from the solution of the LQR problem specified the commands to the pseudo control variables as linear combinations of the state variables of the augmented perturbation model. A transformed gain matrix was used to specify the pseudo control variables as linear combinations of the state variables, sensor variables, and other variables which were functions of the state and sensor variables. The sideslip state variable was replaced by the lateral acceleration measured at the center of

percussion of the airplane relative to a pivot in the vicinity of the horizontal tail and engine nozzles. The bank angle was replaced by the calculated difference between the airplane turn rate and the ideal turn rate The ideal rate is a function of airplane attitude and velocity.

The effectiveness of the elements of the modified gain matrix was examined at a number of angles of attack. Responses of the perturbation system to step deflections of the control stick and rudder pedals were obtained. Each element of the gain matrix was tested to determine if it could be removed without adversely affecting the airplane responses. Those elements which were determined not to be critical to the airplane's stability and controllability by the pilot were eliminated

The reduced gain matrices obtained in the previous step were used to construct schedules The schedules were specified as piecewise linear functions of angle of attack. The airplane responses using the scheduled gains were checked by simulation at the angles of attack used in the previous step and at several intermediate angles. Because air data measurements may be unreliable near and beyond stall, the schedules were made constant in these flight regimes The signal formed by the difference between the airplane turn rate and the ideal turn rate based on airplane attitude and airspeed was found to be important at all the angles of attack examined However, because it depended on reliable measures of angle of attack, pitch angle, bank angle, and airspeed, it was considered to be unavailable at high angles of attack. A substitute signal was formed by obtaining a derivative of the lateral acceleration signal by means of a second-order differentiating filter. This signal was used at angles of attack above 20°.

The design process outlined above could be applied to the longitudinal perturbation system of the airplane. Given that a suitable control system is developed for the longitudinal axis, the next step in the study would be to perform a piloted simulation study to evaluate the combined control system. Because the addition of thrust-vectoring controls enables controlled flight into the poststall regime, new and unusual piloting techniques may surface to exploit the new capability of the airplane. Modifications of the system to deal with the nonlinear and coupled lateral-directional and longitudinal dynamics are to be expected. These topics are beyond the scope of this report and are being left for future research

Design Details

The previous section briefly outlined the salient features of a proposed procedure for the design of a lateral-directional stability augmentation and control system for a high-performance fighter airplane fitted with thrust-vectoring controls This section expands that discussion and presents each of the points mentioned previously in greater detail.

Mathematical Model

A set of nonlinear differential equations was used to formulate a mathematical model of the six-degree-of-freedom dynamics of an airplane representative of a modern high-performance fighter. The aerodynamic data were approximated by manually fitting a series of linear and low-order-polynomial segments to wind-tunnel data. The data were available for an angle-of-attack range of 0° to 60°. The data were extrapolated to an angle of attack of 90°. The airplane cannot sustain appreciable airspeed at such extreme angles of attack. The aerodynamic forces and moments would be very small in comparison with the forces and moments generated by the thrust-vectoring controls. For this reason and because the present study was not intended to deal with a specific airplane, the data used were considered to be adequate for the present study.

The lift and drag coefficients are depicted in figure 1. The lift curve is composed of a linear portion for angles of attack from 0° to 14°, a quadratic portion from 14° to 42°, and a linear portion from 42° to 90°. This curve is smooth; therefore, the lift-curve slope is a continuous function of angle of attack. The drag coefficient is an exponential function of the lift coefficient at low angles of attack. Between 24° and 60°, the drag coefficient is the product of the lift coefficient and the trigonometric tangent of the angle of attack. Above 60°, the drag coefficient is a quadratic function of angle of attack with a maximum value of 2.0 at 90°.

The pitching-moment coefficient is depicted in figure 2. The pitching-moment curve is composed of a linear portion for angles of attack from 0° to 12°, a quadratic portion from 12° to 20°, and a linear portion from 20° to 90°. This curve is smooth; thus, the C_{m_α} derivative is a continuous function of angle of attack

The effects of horizontal-tail deflections (δ_h) upon the lift and pitching-moment coefficients are depicted in figure 3. The curves shown for $C_{L_{\delta h}}$ and $C_{m_{\delta h}}$ are composed of linear and quadratic functions of angle of attack. The pitch damping coefficient, C_{m_q}, has a constant value of $-10\,6$ $(\text{rad/sec})^{-1}$

The lateral aerodynamic derivatives are depicted in figure 4, and the lateral control derivatives are depicted in figure 5. These derivatives are made up of piecewise linear functions of angle of attack with the exception of $C_{l_{\delta a}}$, which includes a quadratic

segment. The sideslip derivatives C_{l_β} and C_{Y_β} are constant, with values of -0.00225 deg^{-1} and -0.0155 deg^{-1}, respectively. The side-force derivatives C_{Y_p} and C_{Y_r} are 0.

An idealized bidirectional thrust-vectoring nozzle was fitted to each of the airplane engines. Each nozzle was assumed to be capable of changing the direction of the thrust force by 15° in any direction. The operation of the two nozzles to produce moments about each axis of the airplane is depicted in figure 6. Simultaneous deflections of the nozzles in the symmetric plane of the airplane produce a pitching moment (pitching thrust vector), differential deflections in the symmetric plane produce a rolling moment (rolling thrust vector), and simultaneous lateral deflections produce a yawing moment (yawing thrust vector). The thrust force was assumed to pivot about the nozzle location with no change in magnitude. No consideration was made for variations in the aerodynamic coefficients caused by thrust vectoring.

Perturbation Equations

Trim solutions of the mathematical model were found for flight at constant speed and altitude over a range of angle of attack of 0° to 90°. The forces and moments acting on the airplane were balanced by deflections of the horizontal tail, pitching moment produced by thrust vectoring, and engine thrust, as depicted in figure 7. For low angles of attack (less than the stall angle of attack), the pitching moment required to trim the airplane was generated by the horizontal tail. At higher angles of attack for which the horizontal tail alone was unable to trim the airplane, it was supplemented by thrust vectoring. The thrust of the engines was calculated for flight at constant speed and altitude. Sea level standard air density was used for these calculations.

The horizontal-tail deflection, δ_h, the total thrust of the engines, T, the thrust-vectoring angle, $\delta_{v,\text{pitch}}$, and the airspeed, V, of the trimmed airplane model are given in figure 8. At an angle of attack of 90°, the airplane is "standing on its tail" in a hovering condition.

A system of linear perturbation equations for the lateral-directional dynamics of the airplane was calculated for angles of attack throughout the range of 0° to 90°. An example is given in table I. The state variables are the body axis roll and yaw rates, p and r, the bank angle, ϕ, and the sideslip angle, β. The control variables are aileron deflection, δ_a, rudder deflection, δ_r, differential horizontal-tail deflection, δ_D, and the thrust-vectoring controls, $\delta_{v,\text{roll}}$ and $\delta_{v,\text{yaw}}$. The lateral acceleration of the center of gravity ($a_{y,\text{cg}}$) is included in the perturbation system.

The open-loop eigenvalues of the perturbation system are plotted on the complex s-plane in figure 9. For low angles of attack, the eigenvalues are configured in the traditional roll, spiral, Dutch roll arrangement. The roll and spiral modes are first order, with the eigenvalue of the spiral mode being near the origin and the eigenvalue of the roll mode being far from the origin on the negative real axis. The complex eigenvalue shown represents the damped oscillatory Dutch roll mode. At an angle of attack of approximately 20°, the roll and spiral modes are replaced by a second-order mode, which is indicated on figure 9 by the real eigenvalues merging to form a complex pair. This mode is commonly termed the "coupled roll-spiral" mode. At an angle of attack of 40°, this mode becomes very lightly damped. The effects of this mode might be recognized by the pilot to be "wing rock."

It is difficult to describe the modes of the airplane in terms of the traditional modes (roll, spiral, etc.) when the angle of attack exceeds 20°. In this report, the mode corresponding to the complex eigenvalues which lie on the locus which originates with the merger of the roll and spiral eigenvalues is termed the "roll-spiral" mode. The other second-order mode is termed the "Dutch roll" mode.

The magnitudes of the lateral-directional eigenvalues and the damping ratios of the second-order modes are plotted as functions of angle of attack in figure 10. For complex modes, the magnitudes shown are the undamped natural frequencies of the modes. For real modes, the magnitude is the inverse of the time constant of the modes.

The natural frequency of the Dutch roll mode is less than 1.5 rad/sec for angles of attack greater than 15° and less than 1.0 rad/sec for angles of attack near 25° and greater than 77°. The damping ratio varies between 0.25 and 0.85 with the greater values occurring between 25° and 45°. The maximum damping factor ($\xi\omega_n$) of 1.22 sec^{-1} occurs at an angle of attack of 40°. The damping factor is less than 0.8 sec^{-1} for angles of attack between 5° and 26° and greater than 45°.

For angles of attack less than 18°, the roll and spiral modes are distinct first-order modes. The time constant ($|\lambda|^{-1}$) of the roll mode increases with increasing angle of attack, whereas the time constant of the sprial mode decreases. Both time constants approach 2 sec at an angle of attack of approximately 18°. For angles of attack greater than 18°, the roll and spiral modes are replaced by a second-order roll-spiral mode, which has a minimum damping ratio of 0.094 at 40°.

Pseudo Control Variables

The lateral-directional perturbation equations obtained in the preceding section include the effects of five independent control variables. The pilot can only be expected to be able to manipulate a maximum of two manual controllers for lateral-directional control of the airplane. These are typically lateral control stick and rudder pedal movements. Several sensed variables must be fed into the flight control computers to stabilize the airplane and to modify its responses in order to meet mission requirements and have acceptable handling qualities The combination of a large number of inputs and a large number of controlled outputs results in a sizable quantity of signal paths which could be implemented through the control computers. In addition, the variation of the effectiveness of the aerodynamic and thrust-vectoring controls with changing flight condition makes the incorporation of gain-scheduling algorithms into the flight control computers necessary. The resultant complexity of the final system could easily become quite unwieldy.

The approach taken in the present study is to systematically interconnect the controls, so that their activity is based upon two "pseudo" control variables within the flight control computers The relationships between the controls and the pseudo controls are specified by schedules which are dependent upon flight condition. The schedules are developed from calculations based upon the effectiveness that each control has on the lateral-directional modes of the airplane. Incorporation of the schedules into the perturbation equations results in a modified system of perturbation equations. The modified system has two pseudo control variables for inputs, whereas the original system had five control inputs. The control interconnect schedules result in coordination among the original control variables.

Before specifying the control interconnect schedules, it would be informative to examine the relative effectiveness of the five controls The relative control effectiveness measure of reference 1 was applied to the perturbation dynamic equations. This measure provides some insight into how the effectiveness of the different controls varies with changing flight condition. A control which has a large effect on a given mode is a logical candidate for use in (1) exciting that mode in response to pilot inputs and (2) modifying the frequency and damping of the mode by means of feedback loops. However, if the control must be used on a second mode, such usage will likely disturb the first mode.

The relative effectiveness of each control upon the Dutch roll mode is presented in figure 11 as a function of angle of attack. The significance of this figure is that it quantitatively represents the ability of each control, relative to the total set of controls, to affect the Dutch roll mode. For angles of attack less than 16.5°, the Dutch roll mode is more strongly affected by deflections of the rudder than it is by any one of the other controls. For angles of attack greater than 16.5°, yawing thrust vector is the most effective. The rudder loses effectiveness at high angles of attack because of a small $C_{n_{\delta r}}$ derivative and low dynamic pressure. The thrust-vectoring controls become powerful at high angles of attack because of the high engine thrust level At an angle of attack of 16.5°, the ailerons, rudder, and yawing thrust vector are equally effective upon the Dutch roll mode because the ailerons have an adverse yaw characteristic and because the Dutch roll mode involves large rolling motions about the longitudinal body axis of the airplane. The relative effectiveness of the rolling thrust vector reaches a level of 0 6 at an angle of attack of 70° (not shown) but remains less effective than the yawing thrust vector. At such an extreme angle of attack, the Dutch roll mode is characterized mainly by production of sideslip angle when the airplane rotates about its longitudinal axis. The rolling thrust vector is weak because of the close spacing of the engines, whereas the yawing thrust vector is much stronger because of the long moment arm between the airplane center of gravity and the engine nozzles. The strong yawing moments couple through the product of inertia, I_{XZ}, to excite the Dutch roll mode to a greater extent than the rolling moments, which act more directly on the mode.

The relative effectiveness of the controls upon the roll and spiral modes is depicted in figure 12. At low angles of attack, aileron control is the most effective because it can produce the largest rolling moment. At higher angles of attack (up to approximately 16°), the rudder is the most effective because yawing moments are required to rotate the airplane about the longitudinal stability axis (the wind vector) and because the ailerons possess an adverse yaw characteristic At angles of attack greater than 16°, the yawing moment produced by the thrust-vectoring control is most effective in exciting the roll and spiral modes.

The above discussion implies that the flight control system should use the aerodynamic control surfaces during high-speed flight at low angles of attack and the thrust-vectoring controls during low-speed flight at high angles of attack. The controls need to be blended, so that the most effective combination is always in use. In addition, it is desirable that each control channel (lateral and directional) create a minimum disturbance on the other channel. To

accomplish these objectives, the control-mixing technique of reference 1 has been used

The control-mixing technique is a method for calculating proportional deflections of the controls, so that selected modes are affected to the maximum extent possible while maintaining a minimum disturbance of the modes which are to remain decoupled. This trade-off is accomplished by means of an algebraic optimization problem whose solution is the desired control combination. Details about the technique may be found in reference 1.

The control-mixing technique was applied to the perturbation system to find two sets of control interconnects The first set has maximum effect upon lateral airplane motions with minimum effect upon directional motions The second set has maximum effect upon directional airplane motions with minimum effect upon lateral motions The control interconnects were calculated for the airplane with and without thrust-vectoring controls.

The control interconnects calculated for lateral control (maximum excitation of the roll and spiral modes with minimum excitation of the Dutch roll mode) using only aerodynamic controls are presented in figure 13. At low angles of attack, lateral control is accomplished by simultaneous deflections of the ailerons and differential tail to produce rolling moments At higher angles of attack, the rudder is used to produce the yawing moments required to roll the airplane about the longitudinal stability axis The ailerons reverse sign at angles of attack above 20°, so that their adverse yaw characteristic is utilized in aiding the rudder in producing yawing moments. In this region, the differential tail is producing rolling moments to cancel the rolling moments produced by the ailerons

The control interconnects calculated for lateral control using thrust-vectoring controls in addition to aerodynamic controls are presented in figure 14. Below an angle of attack of 15°, the interconnects are similar to those presented in figure 13. The aerodynamic controls are much more effective than the thrust-vectoring controls when the airplane is trimmed in this region because of the high dynamic pressure The yawing thrust vector, $\delta_{v,\text{yaw}}$, becomes effective between angles of attack of 10° and 20°. Above 20°, it overpowers the aerodynamic controls For this reason, the deflections of the aerodynamic controls are very small, whereas $\delta_{v,\text{yaw}}$ operates at full authority.

The calculated interconnects, if implemented in the airplane flight control computers, result in optimal decoupling of the airplane modes The calculated interconnects are useful as guides in specifying practical control interconnect schedules. Interconnect schedules were developed for lateral airplane control. These schedules, presented in figure 15, were manually fitted to the curves of figures 13 and 14. The schedules for the aerodynamic controls were made to be functions of angle of attack and are based upon the curves of figure 13. The curves of figure 14 were not used here, so that the aerodynamic controls would remain active at high angles of attack. A loss of thrust will not necessarily eliminate all possibility of controlling the airplane. The thrust-vectoring controls were scheduled as functions of effective airspeed to approximate the curves of figure 14. Airspeed was used as the scheduling quantity instead of angle of attack, so that the airplane would retain effective controls if it should acquire a low angle of attack while at low airspeed during maneuvering flight. Alternatively, the thrust-vectoring controls could have been scheduled as functions of dynamic pressure.

The interconnects calculated for directional control (maximum excitation of the Dutch roll mode with minimum disturbance of the roll and spiral modes) using the aerodynamic controls are presented in figure 16 At low angles of attack, directional control is accomplished by the rudder. Between 10° and 20°, a combination of the rudder, ailerons, and differential tail is used. The deflections are in the crossed-control sense: rudder for nose-left moment, and ailerons and differential tail for right-wing-down moment. For angles of attack greater than 20°, simultaneous aileron and differential tail deflections are used to produce a rolling moment about the airplane longitudinal axis

The interconnects calculated for directional control using the thrust-vectoring controls in addition to the aerodynamic controls are presented in figure 17. These interconnects are very similar to those presented in figure 16 The utilization of the rolling thrust vector gradually increases at angles of attack from 10° to 60°. This control is limited in its ability to generate rolling moments because of the close spacing of the engines. The horizontal tail retains the ability to generate rolling moments at high angles of attack. Therefore, the transition between aerodynamic and thrust-vectoring controls is spread over a wide range of angle of attack.

Control interconnect schedules were developed for directional airplane control. These schedules, presented in figure 18, were manually fitted to the curves of figures 16 and 17. The aerodynamic controls were scheduled as functions of angle of attack and are based on the curves of figure 16 The thrust-vectoring controls were scheduled as functions of effective airspeed and are based on the curves of fig-

ure 17 The schedule for the rolling-moment thrust vector, $\delta_{v,\text{roll}}$, was adjusted so that full authority was used for airspeeds ranging from zero to just greater than the stall speed.

The schedules for the aerodynamic controls given in figures 15 and 18 require angle-of-attack sensor data ranging from zero to a value less than the stall angle of attack. At higher angles of attack, a stall sensor could be used. The schedules for the thrust-vectoring controls require airspeed sensor data for airspeeds above the stall speed. For slower speeds, accurate data are not required.

This section has discussed the development of control interconnect schedules which specify how the five airplane controls need to be coordinated to result in decoupled (as much as possible) lateral and directional control Two "pseudo" control variables can now be defined within the flight control computers The first pseudo control variable, v_{lat}, acts through the schedules of figure 15 to deflect the controls in the proportions required to primarily excite the roll and spiral modes In the examples of reference 1, this pseudo control variable was treated as if it were a lateral deflection of the control stick In these examples, the airplane model responded to step inputs with a smooth buildup of bank angle and exhibited no evidence of adverse yaw motions The second pseudo control variable, v_{dir}, acts through the schedules of figure 18 to primarily excite the Dutch roll mode. In reference 1, this pseudo control variable was treated as if it were a deflection of the rudder pedals. The airplane model responded to step rudder pedal inputs with improved sideslip behavior accompanied by less rolling motion compared with the response to rudder surface deflections alone.

The perturbation system equations were combined with the control interconnect schedules to produce the modified perturbation system shown in figure 19. A numerical example is given in table II. The pseudo control variables are the control variables of the modified system. The control system design described in the remainder of this report is based upon the modified perturbation system.

Linear Quadratic Regulator

The airplane mathematical model used in the present study has poor stability at high angles of attack The airplane motions must be measured, and the controls must be driven by these measurements to improve stability. The design of a stability augmentation system involves the determination of the sensor complement which can make the required measurements and the development of control laws which transform the sensor signals into control variable commands Also, the control laws must translate the motions of the pilot's controllers into control activity which results in acceptable airplane behavior. Although the results of reference 1 indicate that the control stick should be connected to v_{lat} and the rudder pedals should be connected to v_{dir}, this arrangement may not be appropriate in general In order to determine suitable gains to direct the sensor and pilot controller signals to the pseudo control variables, the linear quadratic regulator (LQR) techniques of reference 2 were applied to the modified perturbation system. This section describes the formulation of the LQR problem used in the present study. Following sections describe the process of making a more practical implementation of the control laws.

The LQR technique finds a matrix of feedback gains which specify the control variables of a linear system as linear combinations of its state variables The gains are calculated to minimize a quadratic function of system variables, which may include state variables, output variables, control variables, and combinations of these. The quadratic performance index is constructed to effect a trade-off between the magnitudes of undesirable system responses and the control variables. The result of the LQR technique is a gain matrix which makes the closed-loop system stable and which regulates the system to continually seek the nominal operating condition.

The objectives of the LQR design for the present study are (1) to improve the lateral-directional stability of the airplane, (2) to provide acceptable control characteristics by using lateral control stick and rudder pedal motions, and (3) to coordinate turning maneuvers. The third objective may be relaxed during operation at extremely high angles of attack, at which the airplane is not likely to be operated for sustained periods of time. The formulation of the LQR problem used to meet these objectives is described in this section. This approach closely parallels the formulation used in the development of the control configured vehicle (CCV) system reported in reference 3

A number of auxiliary equations were appended to the modified perturbation system. The added equations were lateral and directional pilot command models, lateral and directional reference response models, differences between the airplane motions and the reference models, and an integration over time of the lateral acceleration. These auxiliary equations are schematically depicted in figure 20.

The pilot command models are first-order systems which are driven by Gaussian white noise. The break frequency of each is 1 rad/sec These models represent lateral control stick, δ_s, and rudder pedal,

δ_{rp}, motions which are limited to a bandwidth of 1 rad/sec. Since the pilot controller motions are state variables, the LQR design technique calculates the pilot controller gains.

The reference response models are first-order systems which are driven by the pilot command models. The break frequency of each is 5 rad/sec. These models respond to pilot commands to generate reference signals against which the airplane responses can be compared

The first reference response model, p_m, is the ideal airplane roll rate about the stability axis. The actual stability axis roll rate, p_s, is a function of the body axis roll rate, p, the body axis yaw rate, r, and the angle of attack, α. The difference between the actual roll rate and the ideal roll rate is calculated by

$$y_1 = p_s - p_m = p\cos\alpha + r\sin\alpha - p_m \qquad (1)$$

During coordinated turns, the turn rate is a function of the component of the lift vector which is directed toward the center of the turn. This force is balanced by the centrifugal force of the airplane following a curved trajectory. This balance is not achieved during uncoordinated turns because of side forces, principally caused by sideslip, acting on the airplane The difference between the actual turn rate and the turn rate expected for a coordinated turn can be defined as the "turn coordination error," T_{ce}, as follows:

$$T_{ce} = \frac{g}{V}\phi\cos\theta - (r\cos\alpha - p\sin\alpha) \qquad (2)$$

where

θ pitch angle

ϕ bank angle

V velocity

g gravitational acceleration constant

A variable which is interpreted as the rate of change of sideslip angle is defined in reference 3. This variable and T_{ce} are calculated by identical formulas.

For the present study, the response of the directional reference response model, r_m, to rudder pedal inputs was considered to be the desired response of the turn coordination error. The difference between the actual and the desired turn coordination error is calculated by

$$y_2 = T_{ce} - r_m = \frac{g}{V}\phi\cos\theta - (r\cos\alpha - p\sin\alpha) - r_m \qquad (3)$$

The integral over time of the lateral acceleration of the airplane is a measure of the long-term error of turn coordination. If a directional control is applied and the wings are held level, the force produced by sideslip causes the airplane to execute a flat turn. The lateral acceleration and the turn rate are related through velocity. The difference between the lateral acceleration, a_y, and the "ideal" acceleration, Vr_m, is integrated over time to yield the desired measure as follows.

$$y_3 = \int (a_y - Vr_m)dt \qquad (4)$$

The value of the lateral acceleration used here is taken at the location of the lateral accelerometer, which is discussed in a later section of this report.

The performance index for the LQR problem is the integral over time of a weighted sum of squares of (1) the differences between the airplane responses and the idealized responses (y_1, y_2, and y_3) and (2) the pseudo control variables, as follows:

$$J = \int (50y_1^2 + 2500y_2^2 + 0.1y_3^2 + 500v_{lat}^2 + 500v_{dir}^2)dt \qquad (5)$$

The weights used in equation (5) are roughly equivalent to the weights used in reference 3. The LQR techniques of reference 2 were used to find the "feedback" matrix of gains which minimize the performance index subject to the dynamics of the modified perturbation system and the auxiliary equations, which can be represented as

$$\dot{\mathbf{x}} = \mathbf{Ax} + \mathbf{Bv} \qquad (6)$$

where

A matrix of state variable coefficients

B matrix of control variable coefficients

v pseudo control vector consisting of v_{lat} and v_{dir}

x state vector consisting of (1) airplane state variables (p, ϕ, r, β), (2) pilot command model states (δ_s, δ_{rp}), (3) reference model states (p_m, r_m), and (4) integrated error of lateral acceleration (y_3)

An example solution of the LQR problem is given in table III. The solution is a matrix of gains which specify the pseudo control variables (v_{lat} and v_{dir}) as linear combinations of all the state variables. Since the state variables include the pilot command models and reference state models, the matrix includes "feedforward" gains for the pilot controllers.

Feedback Variable Change

The sensor package carried onboard the airplane is assumed to include rate gyros to measure the body axis roll rate (p) and the yaw rate (r), a linear accelerometer oriented to measure the lateral acceleration (a_y), and an attitude gyro to measure the bank angle (ϕ). The lateral accelerometer is positioned forward of the center of gravity at the "center of percussion" of the airplane with respect to forces applied at the tail Considering only the mass and inertia of the airplane, application of control forces causes it to rotate about the center of percussion. The location of the center of percussion is the distance l_{cp} forward of the center of gravity The formula for calculating l_{cp} is

$$l_{cp} = \frac{I_Z}{l_t m} \tag{7}$$

where

m	mass of airplane
I_Z	moment of inertia about vertical axis
l_t	distance between center of gravity and tail controls

The accelerometer, with this positioning, principally reacts to aerodynamic side forces (in this example, caused by sideslip acting through the aerodynamic derivative C_{Y_β}) and has a minimum direct reaction to control motions. This location was chosen to avoid possible stability problems caused by a loop from control deflection to side force to accelerometer response.

A measurement vector ($\mathbf{y}_m$) was constructed of the known state variables (δ_s, δ_{rp}, p_m, r_m, and y_3), the sensed angular rates (p and r), the sensed lateral acceleration (a_y), and the calculated value of the turn coordination error (T_{ce}). This vector is a linear function of the state vector of the perturbation system ($\mathbf{x}$) and the pseudo control vector ($\mathbf{v}$) and has the following form:

$$\mathbf{y}_m = \mathbf{H}\mathbf{x} + \mathbf{G}\mathbf{v} \tag{8}$$

The solution of the LQR problem found in the preceding section has the following form:

$$\mathbf{v} = \mathbf{F}\mathbf{x} \tag{9}$$

Combining equations (8) and (9) yields

$$\mathbf{v} = \mathbf{F}_b\mathbf{y}_m \tag{10}$$

where

$$\mathbf{F}_b = (\mathbf{I} + \mathbf{F}\mathbf{H}^{-1}\mathbf{G})^{-1}\mathbf{F}\mathbf{H} \tag{11}$$

The matrix ($\mathbf{F}_b$) is the feedback matrix, which specifies the pseudo control variables as linear combinations of the elements of the measurement vector. Examples are presented in table IV. The values of the elements of this matrix are plotted in figure 21. The data shown are the gains on the measurement vector which cause the controls to act in a manner which satisfies the LQR problem.

The next step of the design process is to identify those elements of the gain matrix which are necessary for the satisfactory operation of the airplane controls. By the elimination of ineffectual gain elements, the mechanization of the control laws in the flight control computers can be simplified.

Gain Element Reduction

The individual gain elements of the feedback matrix were deleted or retained based upon the effects of their presence on simulated transient responses. The modified perturbation system was used to obtain the airplane responses to step lateral stick and rudder pedal movements. Reduced gain matrices were obtained at angles of attack of 10°, 20°, 30°, and 60°. This section describes the process of gain element reduction and discusses the reduced-gain matrices.

Simulated responses to step lateral stick and rudder pedal movements using the full feedback matrices were obtained. When the stick was held off center, the airplane tended to return to a wings-level attitude after a long period of time This was caused by the feedback of y_3 (the integral of lateral acceleration). Since the perturbation model did not include increasing pitching moment, which is required for turn coordination, the airplane model lost altitude when banked As a result, the simulation showed a buildup of sideslip and, consequently, lateral acceleration. The control system acted to drive the lateral acceleration to zero by causing the airplane to return to level flight Since this behavior is unacceptable in maneuvering flight, the feedback gains for y_3 were deleted. These gains could be reintroduced into the control system as part of a more comprehensive system design. For the present study, these gains were not considered further.

Simulated responses to step lateral stick and rudder pedal movements were obtained with the controller crossfeeds (δ_s to v_{dir} and δ_{rp} to v_{lat}) and the reference model crossfeeds (p_m to v_{dir} and r_m to v_{lat}) deleted. The elimination of these crossfeeds caused no significant deterioration of the airplane responses. These crossfeeds were not considered further in the present study.

The elements of the feedback gain matrix which operate on signals derived from airplane motion sensors (p, T_{ce}, r, and a_y) were examined next. Table IV

presents the measurement feedback gain matrices for the four angles of attack presently being considered The gain elements which are retained after the elimination process are given in boldface type. In general, as the angle of attack is increased, more feedback loops must be utilized to control the airplane.

For an angle of attack of 10°, most of the feedback gains were eliminated because either they had little discernible effect on the airplane responses or the effect was adverse. The only feedback gain element that was retained closed the loop from T_{ce} to v_{dir} This gain improves Dutch roll mode damping and causes a coordinating rudder deflection, which is desirable in turning flight.

For an angle of attack of 20°, additional gains were used to close the loops from the yaw rate (r) and sensed lateral acceleration (a_y) to the lateral pseudo control variable (v_{lat}) Both feedbacks improved the Dutch roll damping, with the a_y loop having the greater effect. For a step rudder pedal deflection to the left, the airplane transitions smoothly to a steady right sideslip (nose-left) with a small right-wing-down bank angle. For a step lateral stick deflection, the airplane rolls smoothly to a constant bank angle with a time constant of approximately 4 sec. The airplane does not continue to roll because of the presence of the coupled roll-spiral mode and the yaw rate feedback The pilot must hold a stick deflection toward the turn in order to maintain a constant bank angle. The airplane returns to a wings-level attitude when the stick is released. Deletion of the yaw rate feedback results in a sustained rolling motion because the lateral acceleration feedback drives the controls to reinforce the pilot's roll command This may be objectionable because the pilot must hold a stick deflection away from the turn in order to maintain a constant bank angle. Also, the control power available to right the airplane would be limited. A compromise value of 0 3 for the yaw rate to v_{lat} gain was selected This is approximately one half of the value given by the LQR problem.

For an angle of attack of 30°, an additional gain element was used to close the feedback loop from the yaw rate (r) to the directional pseudo control variable (v_{dir}). For a step rudder pedal deflection to the left, the airplane transitions smoothly to a steady right sideslip with a small right-wing-down bank angle For a step lateral stick movement, the airplane smoothly rolls to a constant bank angle with a time constant of approximately 25 seconds. The inclusion of the yaw rate to v_{dir} loop causes a rolling moment which lifts the wing on the side toward the turn. As a result, the sideslip angle and the lateral pseudo control variable (v_{lat}) are reduced.

The implementation of the turn coordination error (T_{ce}), used in formulating the measurement feedback matrix in the preceding section, requires measurements of angle of attack, pitch angle, and bank angle. Obtaining these measurements reliably at high angles of attack, particularly near or beyond stall, may be impractical Also, operation near a pitch angle of 90° is likely to cause trouble because of the singularity existing in the Euler angles at this attitude. In order to avoid these problems, a substitute signal for T_{ce} was constructed.

As mentioned in the preceding section, one interpretation of the meaning of T_{ce} is that it is an estimate of the time rate of change of the sideslip angle. The sideslip angle can be estimated from the sensed lateral acceleration of the airplane. For angles of attack of 30° and greater, the turn coordination error (T_{ce}) was replaced by an estimated value of the rate of change of the sideslip angle ($\dot{\beta}_{est}$) by using the following formula

$$\beta_{est} = \frac{s}{(\frac{s}{3}+1)(\frac{s}{6}+1)} \frac{m}{\bar{q}SC_{Y_\beta}} a_y \qquad (12)$$

The first term of the formula is a second-order filter which operates as a differentiator on signal components whose frequencies are less than 3 rad/sec. Higher frequency components are attenuated by the action of the second-order denominator, reducing the sensitivity of the differentiating filter to noise on the accelerometer signal but introducing phase lag, which may cause stability problems. Therefore, the use of this filter is limited to flight at low airspeeds, at which the closed-loop frequencies are low. The break frequencies of the filter denominator were selected from observations of their effects on the simulated airplane responses.

The second term of equation (12) is the ratio between lateral acceleration and the sideslip angle based upon the value of the side-force derivative (C_{Y_β}). With the location of the lateral accelerometer at the center of percussion (discussed in the preceding section), the forces produced by the rudder and yawing thrust vector are not sensed by it. This location prevents objectionable coupling of the Dutch roll and roll-spiral modes.

For an angle of attack of 60°, the solution of the LQR problem resulted in no feedback of yaw rate (r) to the directional pseudo control variable (v_{dir}). However, a value of 0 3 for this gain was inserted into the gain matrix to obtain consistency with the matrix obtained for an angle of attack of 30° and to remove the necessity of scheduling gains while the airplane is stalled. The air data measurements necessary for the calculation of $\dot{\beta}_{est}$ (eq (12)) probably cannot

be reliably obtained at extreme angles of attack Therefore, a lower limit of 50 m/sec was chosen for use in the calculation For flight at airspeeds less than 50 m/sec, the following formula was used:

$$\beta_{\text{est}} = \frac{s}{(\frac{s}{3}+1)(\frac{s}{6}+1)} \frac{2m}{50^2 \rho S C_{Y_\beta}} a_y \qquad (13)$$

The gain elimination process, discussed in this section, reduced the number of elements of the measurement vector feedback matrix from the original 18 to the current 8. The cross coupling of the pilot controllers and the ideal rate response models was eliminated The feedback of the roll rate and the time integral of the lateral acceleration were also removed The feedback of the turn coordination error to the directional pseudo control was found to be necessary at each of the angles of attack examined. This signal was replaced by an estimate of the rate of change of the sideslip angle at high angles of attack. Also at high angles of attack, the lateral acceleration was fed to the lateral pseudo control variable, and the yaw rate was fed to both pseudo control variables. The next step of the design process is to construct schedules which smoothly vary the gains as needed for changing flight condition.

Gain Schedules

In the preceding section, it was determined which gains generated by the solution of the LQR problem are necessary for acceptable stability and control of the airplane at angles of attack of 10°, 20°, 30°, and 60° In this section, this information is used in conjunction with the calculated gains given in figure 21 to construct gain schedules The schedules, along with the points examined in the preceding section, are given in figure 22. Those gains which were eliminated for all four angles of attack examined in the previous section are ignored in this section The remaining gains are scheduled as piecewise linear functions of angle of attack. The schedules generally follow the data of figure 21 with some deviations resulting from the gain elimination process of the preceding section.

The calculated gains for the lateral stick deflection (δ_s) and the roll rate model (p_m) to the lateral pseudo control variable (v_{lat}) are given in figure 21(a). At low angles of attack (high airspeed), the gain on the roll rate model dominates. The pilot commands are filtered to limit the bandwidth of his stick motions which reach the controls At high angles of attack (low airspeed), the gain on the stick deflections dominates. Here the airplane is slow to respond to control, as is indicated by the small magnitudes of its eigenvalues. Therefore, the pilot stick motions are passed to the controls relatively unfiltered. The schedules chosen for these gains are given in figure 22(a). At an angle of attack of 0°, the gain on the stick is 0.2, and the gain on the roll rate model is 0 8. At an angle of attack of 20°, the gain on the stick is 0 8, and the gain on the roll rate model is 0 2. These gains are varied linearly at angles of attack between 0° and 20° and are constant at angles of attack beyond 20°.

The calculated gains for the rudder pedal deflection (δ_{rp}) and the yaw rate model (r_m) are given in figure 21(b). These gains are nearly constant with changing angle of attack. Each has a value of approximately 0.5. These gains and the yaw rate model dynamics were combined to form a lag-lead filter as follows:

$$v_{\text{dir}} = \frac{\frac{s}{10}+1}{\frac{s}{5}+1} \delta_{\text{rp}} \qquad (14)$$

This filter passes the low-frequency components of the rudder pedal commands (less than 5 rad/sec) directly to the controls. The high-frequency components (greater than 10 rad/sec) are attenuated by 6 dB

The calculated gain from the turn coordination error (T_{ce}) to the directional pseudo control variable (v_{dir}) is given in figure 21(c). This gain varies between 1 2 and 1 8. A constant value of 1.4 was chosen As discussed in the preceding section, an estimated value of the rate of change of the sideslip angle ($\dot{\beta}_{\text{est}}$) was substituted for T_{ce} for angles of attack of 20° or greater The transition between the two signals was specified as a linear function at angles of attack between 20° and 30°, as shown in figure 22(b). Simulation tests were conducted at an angle of attack of 15° by using (1) T_{ce} only, (2) $\dot{\beta}_{\text{est}}$ only, and (3) the scheduled mix of the two signals. No significant difference in the responses was noted among the three options.

The calculated gains for the yaw rate (r) feedbacks are given in figure 21(c) Although these gains have values at all angles of attack, the gain elimination process of the preceding section determined that they are effective only at the higher angles The gain schedules are given in figure 22(b). The schedules of the yaw rate gains are based primarily on the results of the preceding section and have little correlation with the calculated gains of figure 21(c). The scheduled gain from yaw rate (r) to directional pseudo control variable (v_{dir}) is linearly varied from 0 to 0.30 over the angle-of-attack range of 20° to 30°. The yaw rate to lateral pseudo control variable (v_{lat}) is linearly varied from 0 to 0.60 over the angle-of-attack range of 10° to 30°. These gains are constant beyond 30°.

The calculated gains for the lateral acceleration (a_y) to the lateral pseudo control variable (v_{lat}) are given in figure 21(d). This gain increases from near 0 to approximately 0.18 over the angle-of-attack range of 10° to 30° and is fairly constant from 30° to 60°. The schedule for this gain is given in figure 22(b). The schedule increases linearly from 0 to 0.16 over the angle-of-attack range of 10° to 25° and is constant beyond 25°. The gain for the lateral acceleration to the directional pseudo control variable (v_{dir}) is set to 0.

Schematic diagrams of the lateral and directional control systems, including representations of the gain schedules and the control interconnect schedules, are presented in figure 23. A small-angle approximation for angle of attack (α) has been applied to the formula for the turn coordination error (T_{ce}) (eq. (2)) to produce the mechanization appearing in figure 23(b). Also, the value of velocity used in the T_{ce} and $\dot{\beta}_{est}$ calculations has been limited to no less than 50 m/sec.

Closed-Loop System Characteristics

The eigenvalue characteristics of the airplane with the control system operating are plotted in figure 24. The absolute values of the eigenvalues and the damping ratios of the second-order modes are presented as functions of angle of attack. These data may be compared with the data of figure 10, which are for the unaugmented airplane.

The natural frequency of the Dutch roll mode is slightly less than 1.5 rad/sec, at angles of attack between 14° and 18° and less than 1.0 rad/sec above 82°. The natural frequency has been increased near stall and in the poststall regime. For angles of attack near 90°, this increase is not present because low dynamic pressure prevents effective signals from the lateral accelerometer The damping ratio of the Dutch roll mode is maintained greater than 0.4, which is an improvement at angles of attack less than 20° and greater than 50°. Between these regions, the damping ratio has been decreased. The damping factor ($\xi\omega_n$) has been increased by at least 70 percent for the data in figure 24.

The coupled roll-spiral mode of the unaugmented airplane does not appear in figure 24. Instead, the spiral mode remains as a distinct first-order mode with a minimum time to half amplitude of 2.7 sec at an angle of attack of 30°. The roll mode couples with the differentiating filter used to generate $\dot{\beta}_{est}$ The coupling occurs at an angle of attack of 24°, which is within the range where the turn coordination error is being replaced by $\dot{\beta}_{est}$. The coupled mode exists up to 46°, and the damping ratio remains greater than 0 95 For angles of attack greater than 46°, the first-order roll mode and the filter mode are again distinct. As the signal from the lateral accelerometer weakens with increasing angle of attack, the eigenvalue of the filter mode returns to its open-loop value.

Airplane responses to pilot controller motions are presented in figure 25. The responses are for the linearized perturbation system with the control system operative. The stability axis roll rate responses to full-throw lateral stick deflection are given in figure 25(a). The roll rates achieved are between 1.25 and 1.60 rad/sec over the angle-of-attack range of 10° to 70°. The responses for angles of attack of 20°, 30°, and 40° have an initial delay of at most 0.30 sec. This is probably a consequence of the presence of the coupled roll-spiral mode in the unaugmented airplane. At angles of attack of 10° and 70°, the delay is not present. In the former instance, the roll and spiral mode are distinct first-order modes with well-separated eigenvalues. The airplane is also being primarily driven through the roll rate model, which has a time constant of 1 sec In the latter instance, the aerodynamic forces and moments are ineffectual because of low dynamic pressure. The airplane primarily responds as a free body under the influence of forces and moments generated by the thrust-vector controls.

The sideslip angle responses to full-throw rudder pedal deflections are given in figure 25(b). For the angle-of-attack range of 10° to 70°, the sideslip angle smoothly builds up with a small overshoot and no apparent oscillations. The sideslip angle achieved increases with increasing angle of attack. Lowering dynamic pressure causes smaller restoring moments, smaller aerodynamic moments, and smaller control moments because of smaller lateral accelerometer signals An initial delay of at most 0 3 sec is present in each response shown. For an angle of attack of 10°, the sideslip angle decreases after peaking at 2.5 sec because of the airplane rolling "away from the slip " The roll rate can be arrested by applying a lateral stick deflection of approximately 50 percent in the "crossed-controls" sense. For the angle-of-attack range of 30° to 70°, the sideslip angle slowly builds up after the initial transient because of the airplane slowly rolling "into the slip." Lateral stick motions of less than 7 percent in the "coordinated-controls" sense will arrest the roll rate in each of these instances.

Concluding Remarks

A preliminary design study of a lateral-directional control system using thrust-vectoring controls has been conducted. The control system design was based on a mathematical perturbation model of a

high-performance fighter airplane in trimmed flight over a wide range of angle of attack.

Aerodynamic control surfaces and thrust-vectoring controls were scheduled so that they could be driven by separate lateral and directional pseudo controls This was accomplished by calculating combinations of the controls which affected (1) the roll and spiral modes for the lateral pseudo control and (2) the Dutch roll mode for the directional pseudo control. During flight at low angles of attack and high airspeeds, aileron and differential tail movements are used for lateral control, and rudder movements are used for directional control. During flight at high angles of attack (near or beyond stall) and low airspeeds, rudder movements and yawing moments produced by thrust vectoring are used for lateral control. Aileron and differential tail movements and rolling moments produced by thrust vectoring are used for directional control.

State variable feedback gains were obtained from the solution of a linear quadratic regulator (LQR) problem which minimized the difference between airplane angular rates and idealized rate models. The gains were used to calculate a set of sensor variable feedback gains. Of these gains, those which did not exhibit a beneficial effect upon simulated responses to pilot control inputs were eliminated. The remaining gains were scheduled as functions of flight condition

The directional control channel uses a measure of the turn coordination error to improve the damping of the Dutch roll mode. During flight at high angles of attack, this feedback quantity is replaced by an estimate of the time rate of change of the sideslip angle, and yaw rate feedback is added The lateral control channel uses lateral acceleration and yaw rate during flight at high angles of attack Lag-lead prefilters are used on the control stick and rudder pedal signals.

For the unaugmented airplane, the natural frequency of the Dutch roll mode is less than 1.0 rad/sec for angles of attack near 25° and greater than 77°. The damping ratio varies between 0 25 and 0 85. With the lateral-directional control system active, the augmented natural frequency is slightly less than 1 5 rad/sec at angles of attack between 14° and 18° and is less than 1 0 rad/sec above 82°. The damping ratio stays greater than 0 40. The damping factor ($\xi\omega_n$) is increased by the control system at all angles of attack.

For the unaugmented airplane, the roll and spiral modes merge to form a coupled roll-spiral mode for angles of attack greater than 18°. The damping ratio has a minimum value of 0 094 at an angle of attack of 40° With the control system active, the augmented spiral mode remains a distinct first-order mode with a minimum time to half amplitude of 2 7 sec at an angle of attack of 30°. The roll mode interacts with the filter used to estimate the rate of change of sideslip angle (in the directional channel) to form a second-order mode at angles of attack between 24° and 46°. The minimum damping ratio of this coupled mode is 0.964.

Thrust vectoring provides moments necessary for airplane control at extremely high angles of attack. The formation of pseudo control variables results in a system structure which is divided into lateral and directional components. Application of multivariable controls design methodology produces feedback control loops which modify the airplane dynamic modes to make piloted control possible. Simulated responses to step pilot control inputs are stable and well behaved. For lateral stick deflections, peak stability axis roll rates are consistently between 1.25 and 1.60 rad/sec over an angle-of-attack range of 10° to 70°. For rudder pedal deflections, the roll rates accompanying the sideslip responses can be arrested by lateral stick motions of less than 7 percent.

NASA Langley Research Center
Hampton, VA 23665-5225
July 11, 1985

References

1 Lallman, Frederick J *Relative Control Effectiveness Technique With Application to Airplane Control Coordination* NASA TP-2416, 1985.

2 Armstrong, Ernest S · *ORACLS — A System for Linear-Quadratic-Gaussian Control Law Design* NASA TP-1106, 1978

3 Hartmann, Gary L , Hauge, James A , and Hendrick, Russell C *F-8C Digital CCV Flight Control Laws* NASA CR-2629, 1976

TABLE I LINEAR PERTURBATION SYSTEM

$[\alpha = 20°, V = 59$ m/sec (115 knots)$]$

$$\frac{d}{dt}\begin{Bmatrix} p \\ \phi \\ r \\ \beta \end{Bmatrix} = \begin{bmatrix} -1.48 & 0 & 2.43 & -5.92 \\ 1.00 & 0 & 364 & 0 \\ .010 & 0 & -449 & -017 \\ .342 & 156 & -.940 & -112 \end{bmatrix} \begin{Bmatrix} p \\ \phi \\ r \\ \beta \end{Bmatrix} + \begin{bmatrix} 1\,44 & .254 & 2\,35 & 614 & .656 \\ 0 & 0 & 0 & 0 & 0 \\ -.105 & -425 & 039 & -.033 & -1\,67 \\ 001 & 016 & -.005 & 0 & .062 \end{bmatrix} \begin{Bmatrix} \delta_a \\ \delta_r \\ \delta_D \\ \delta_{v,\text{roll}} \\ \delta_{v,\text{yaw}} \end{Bmatrix}$$

$$a_{y,\text{cg}} = -6\,62\beta + [\,030 \quad 501 \quad -104 \quad 0 \quad 954] \begin{Bmatrix} \delta_a \\ \delta_r \\ \delta_D \\ \delta_{v,\text{roll}} \\ \delta_{v,\text{yaw}} \end{Bmatrix}$$

Variable	Unit
p	rad/sec
ϕ	rad
r	rad/sec
β	rad
$a_{y,\text{cg}}$	m/sec^2

Variable	Unit	Range, rad (deg)
δ_a	rad	±0 70(±40)
δ_r	rad	±0.52(±30)
δ_D	rad	±0.35(±20)
$\delta_{v,\text{roll}}$	rad	±0 52(±30)
$\delta_{v,\text{yaw}}$	rad	±0.26(±15)

TABLE II. MODIFIED PERTURBATION SYSTEM*

$[\alpha = 20°;\ V = 59$ m/sec (115 knots)$]$

$$\frac{d}{dt}\begin{Bmatrix} p \\ \phi \\ r \\ \beta \end{Bmatrix} = \begin{bmatrix} -1.48 & 0 & 2.43 & -5\ 92 \\ 1\ 00 & 0 & .364 & 0 \\ .010 & 0 & -.449 & -\ 017 \\ 342 & 156 & -.940 & -\ 112 \end{bmatrix} \begin{Bmatrix} p \\ \phi \\ r \\ \beta \end{Bmatrix} + \begin{bmatrix} -\ 292 & 1.63 \\ 0 & 0 \\ .650 & -.061 \\ -.024 & -\ 001 \end{bmatrix} \begin{Bmatrix} v_{\text{lat}} \\ v_{\text{dir}} \end{Bmatrix}$$

$$a_{y,\text{cg}} = -6\ 62\beta - 1.42v_{\text{lat}} - \ 052v_{\text{dir}}$$

$$\begin{Bmatrix} \delta_a \\ \delta_r \\ \delta_D \\ \delta_{v,\text{roll}} \\ \delta_{v,\text{yaw}} \end{Bmatrix} = \begin{bmatrix} -9.82 & 33\ 0 \\ -30\ 0 & -.024 \\ 6.00 & 14.7 \\ 0 & 19.0 \\ -13\ 9 & 0 \end{bmatrix} \begin{Bmatrix} v_{\text{lat}} \\ v_{\text{dir}} \end{Bmatrix}$$

*Units of measurement are given in table I

TABLE III. LQR STATE VARIABLE FEEDBACK GAINS*

$[\alpha = 20°,\ V = 59$ m/sec (115 knots)$]$

$$\begin{Bmatrix} v_{\text{lat}} \\ v_{\text{dir}} \end{Bmatrix} = \begin{bmatrix} .308 & .128 & -1.44 & .785 \\ -.343 & -.181 & .777 & .139 \end{bmatrix} \begin{Bmatrix} p \\ \phi \\ r \\ \beta \end{Bmatrix} + \begin{bmatrix} .110 & 890 & -.213 & .577 \\ .341 & 244 & .392 & .608 \end{bmatrix} \begin{Bmatrix} p_m \\ \delta_s \\ r_m \\ \delta_{\text{rp}} \end{Bmatrix} + \begin{bmatrix} .0114 \\ .0083 \end{bmatrix} y_3$$

$$p_m = \frac{1}{\frac{s}{5}+1}\delta_s \qquad r_m = \frac{1}{\frac{s}{5}+1}\delta_{\text{rp}} \qquad y_3 = \int (a_{y,\text{cg}} - Vr_m)dt$$

*p_m and r_m in rad/sec; y_3 and V in m/sec; units for other variables are given in table I.

TABLE IV. MEASUREMENT VARIABLE FEEDBACK GAINS*

α, deg	Pseudo control	p, rad/sec	†T_{ce}, rad/sec	r, rad/sec	‡a_y, m/sec^2	y_3, m/sec	p_m, rad/sec	δ_s	r_m, rad/sec	δ_{rp}
10	v_{lat}	−0.016	−0.33	−0.58	−0.022	0.013	**0 38**	**0.62**	0 24	1.02
	v_{dir}	0 050	**−1.51**	−0 04	−0 005	0.004	0.23	−0 32	**0.56**	**0.43**
20	v_{lat}	0 027	0.85	§**−0 78**	**−0.118**	0.011	**0.10**	**0.90**	−0.22	0 57
	v_{dir}	0.054	**−1.16**	−0 33	−0.021	0 008	0.34	0.25	**0 39**	**0.61**
30	v_{lat}	0.175	0 50	**−1 13**	**−0 180**	0 012	**0.15**	**0 85**	−0.22	0.61
	v_{dir}	0.146	**−1.28**	**−0 31**	0 001	0 008	0.28	0 18	**0.45**	**0.55**
60	v_{lat}	0 190	0 76	**−0 59**	**−0 188**	0.013	**0.22**	**0.78**	−0.25	0.45
	v_{dir}	0.117	**−1.40**	#**−0.02**	−0 025	0 006	0.13	0.24	**0.52**	**0.48**

*Gain elements remaining after the elimination process are given in **boldface** type.

†Substitute $\dot{\beta}_{est}$ for T_{ce}. Use equation (12) for $\alpha = 30°$ and equation (13) for $\alpha = 60°$.

‡The lateral accelerometer is located 2.22 m forward of the center of gravity at the center of percussion.

§Gain element was retained after elimination process, but substitute value of 0.3 was used instead of 0.78.

#Value of 0 3 was used for consistency with gains for $\alpha = 30°$.

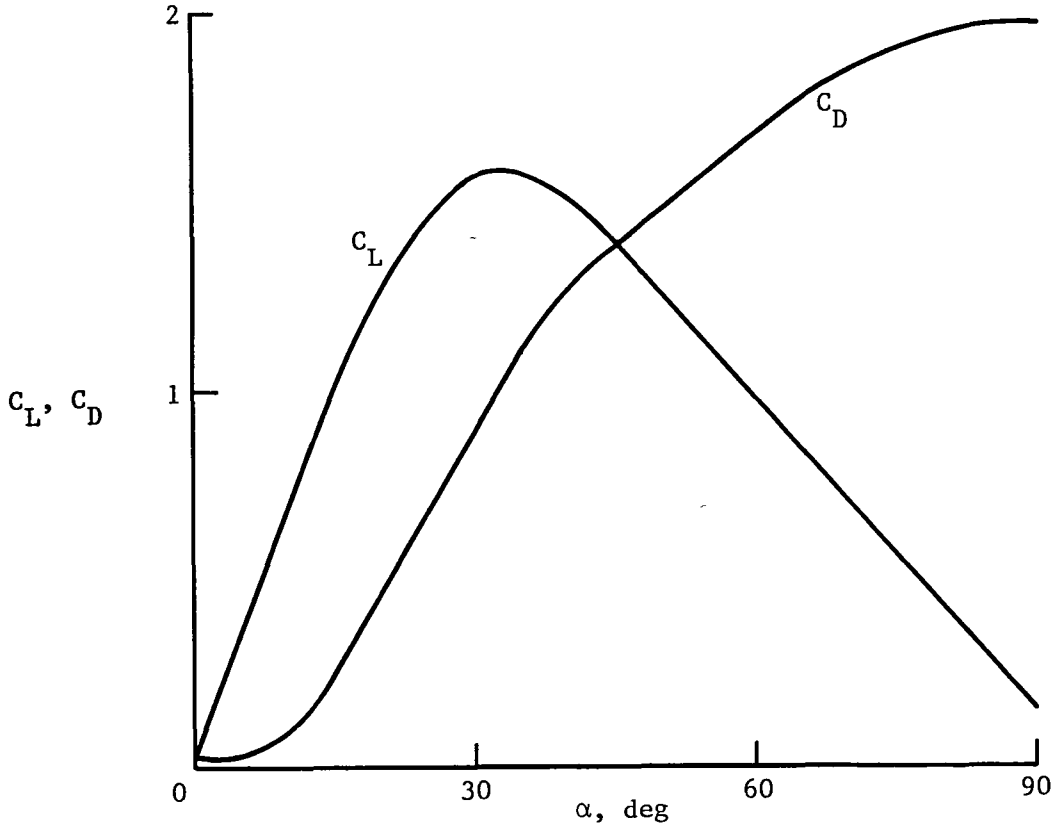

Figure 1 Lift and drag coefficients. $\delta_h = 0°$.

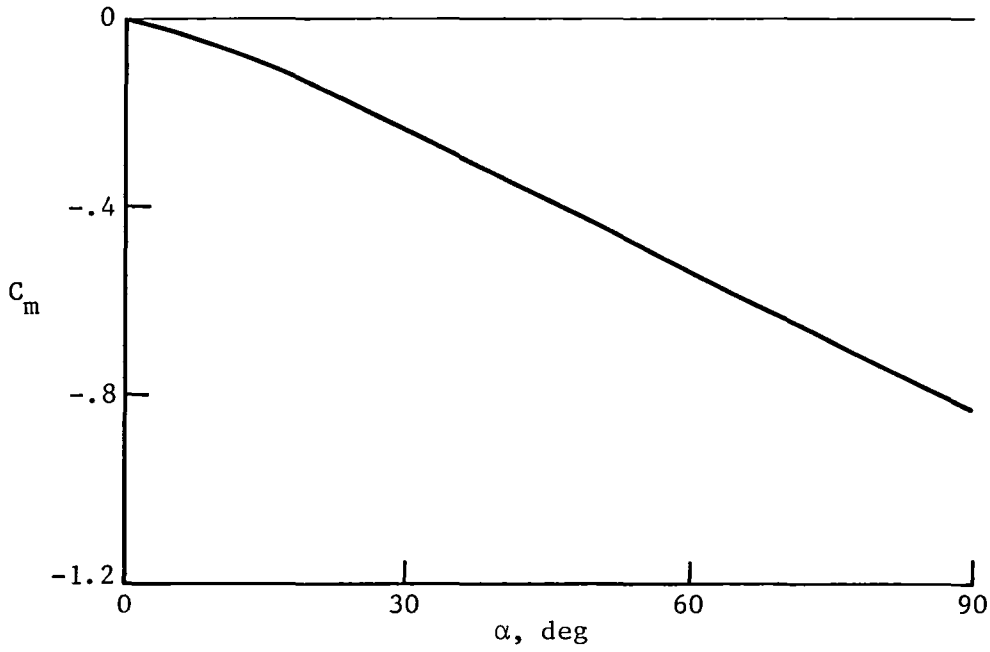

Figure 2. Pitching-moment coefficient. $\delta_h = 0°$.

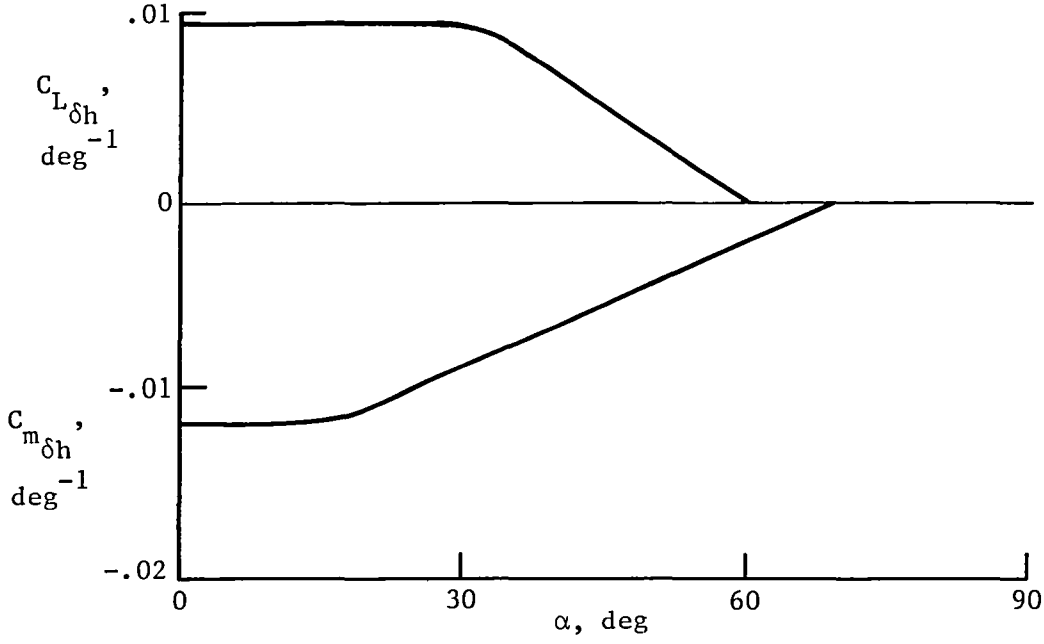

Figure 3 Horizontal-tail coefficients

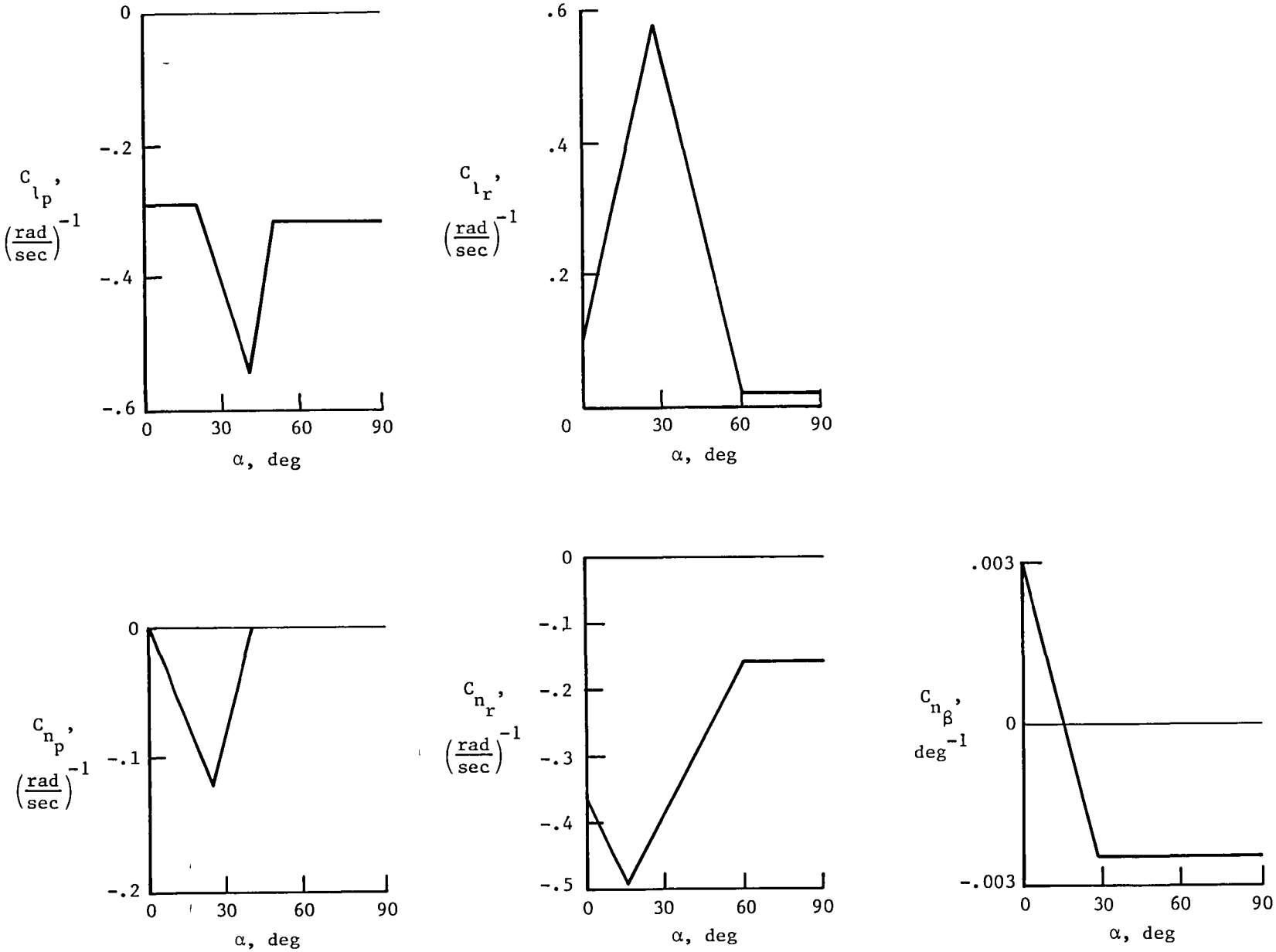

Figure 4. Lateral aerodynamic derivatives.

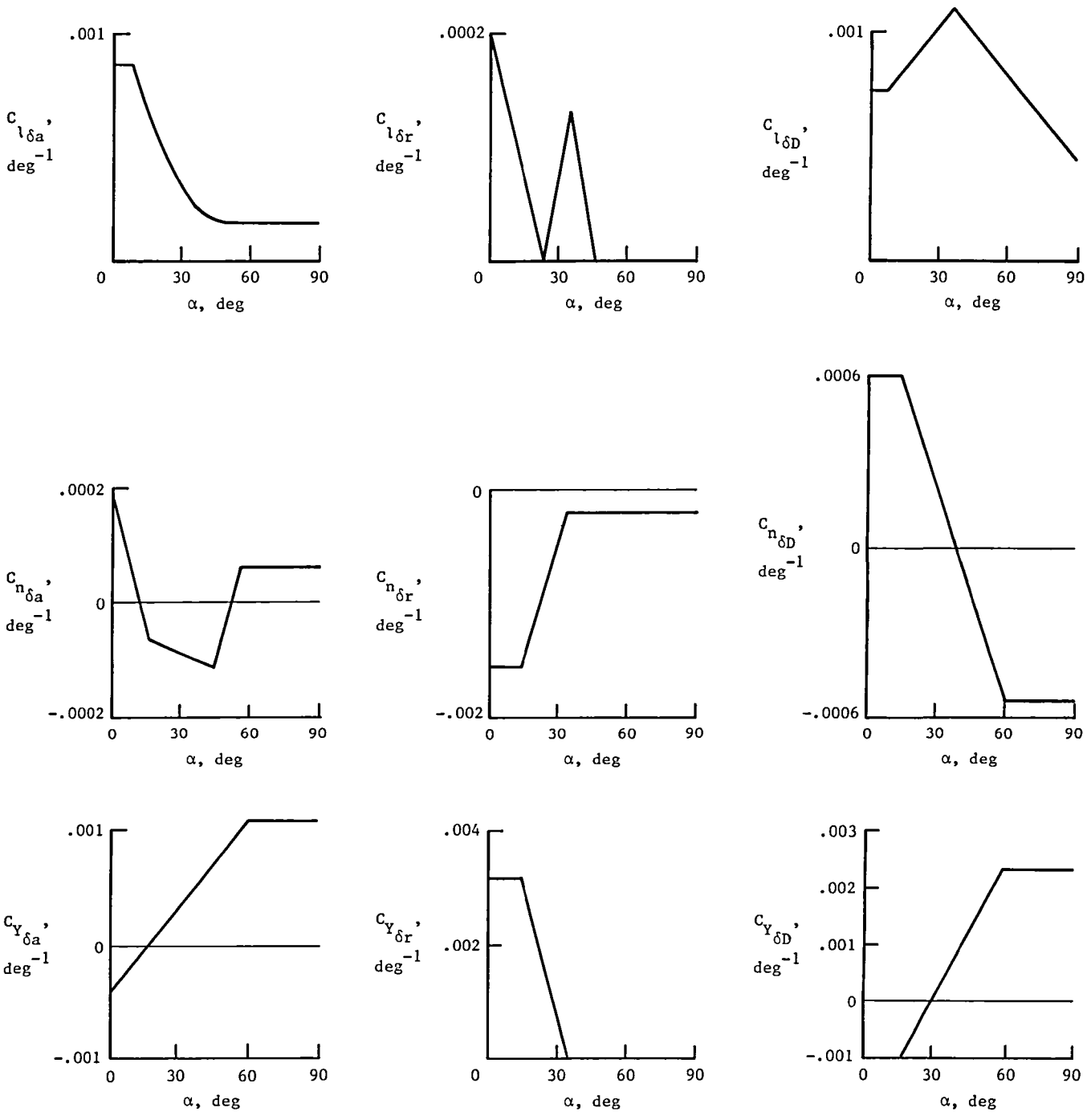

Figure 5. Lateral control derivatives

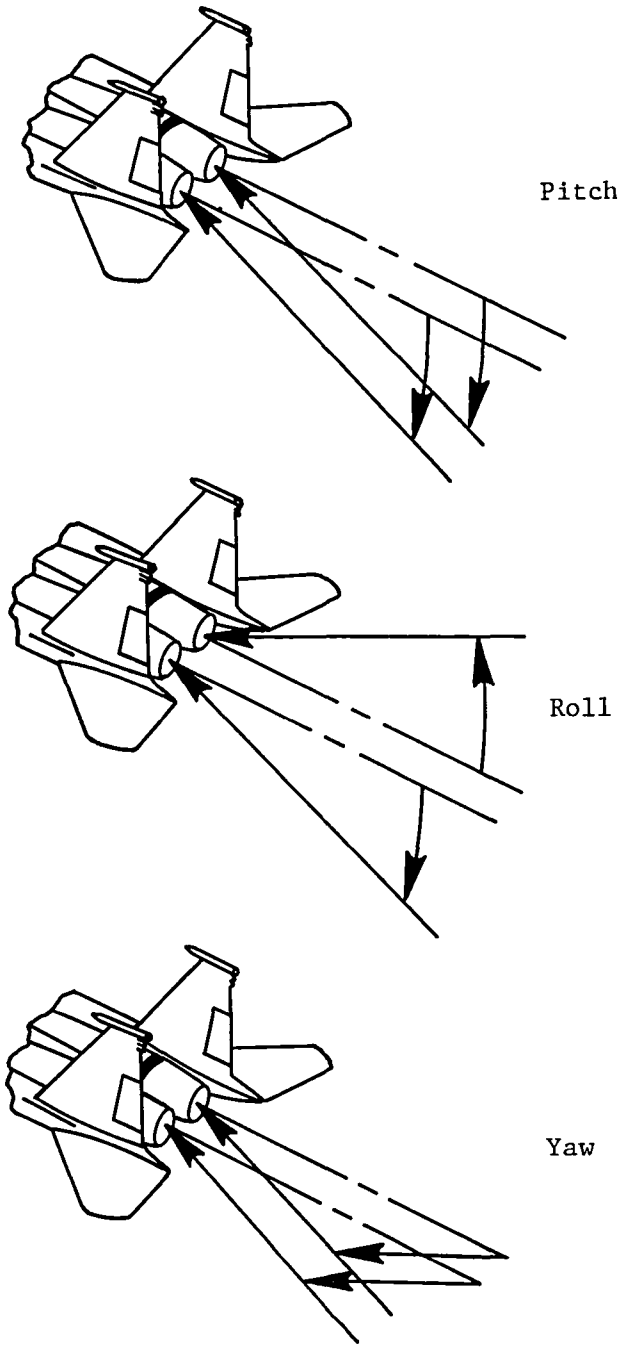

Figure 6 Thrust-vector control moments.

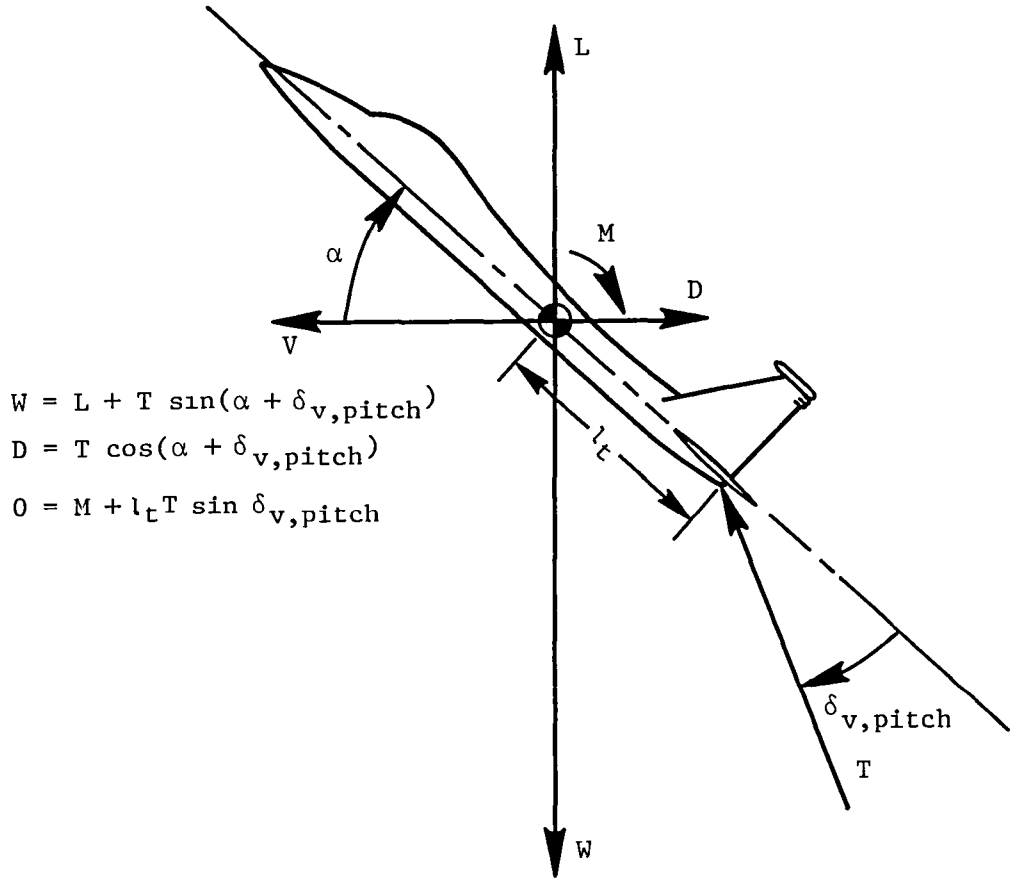

Figure 7 Longitudinal trim.

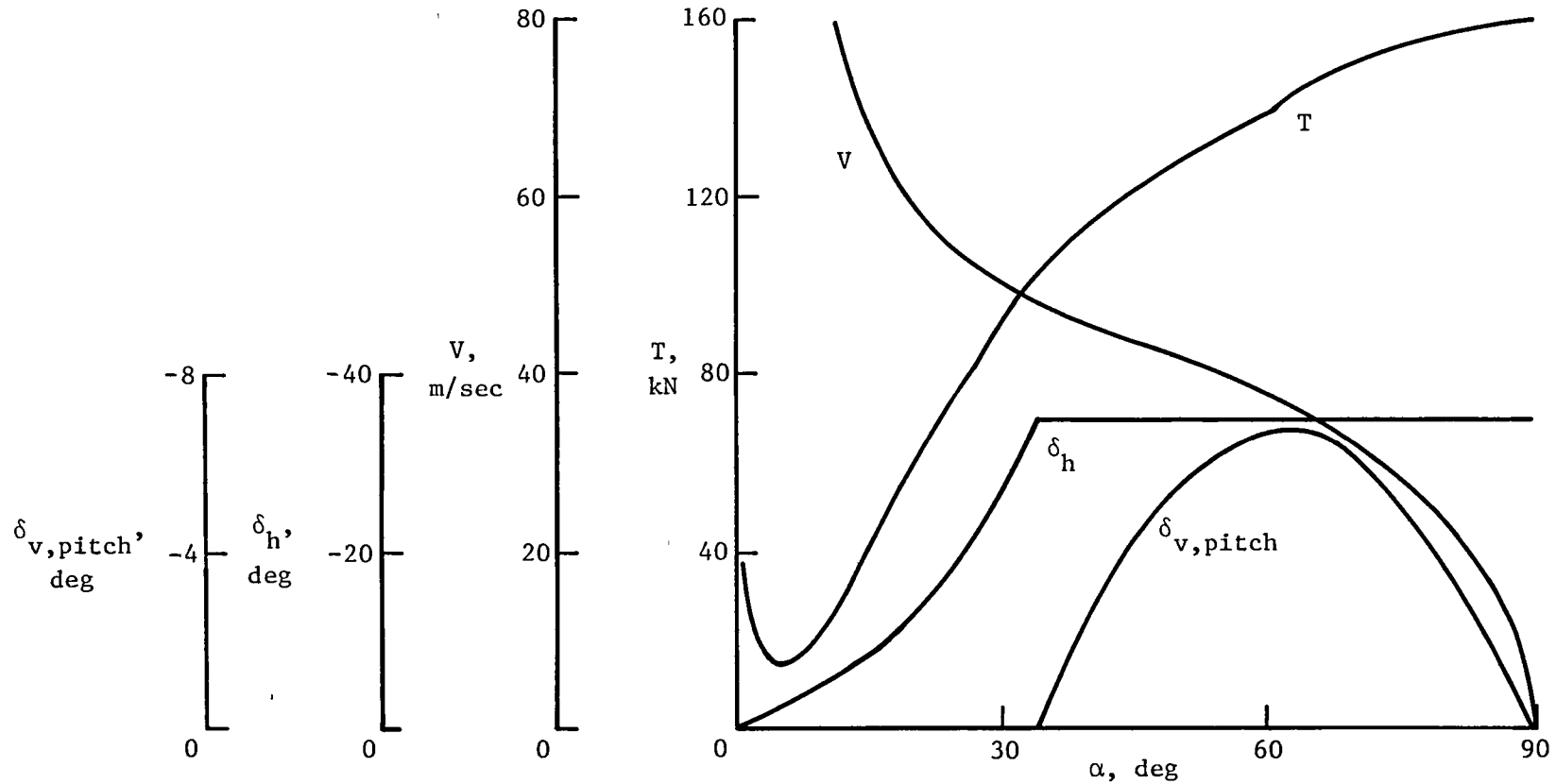

Figure 8. Trim conditions. $\gamma = 0°$.

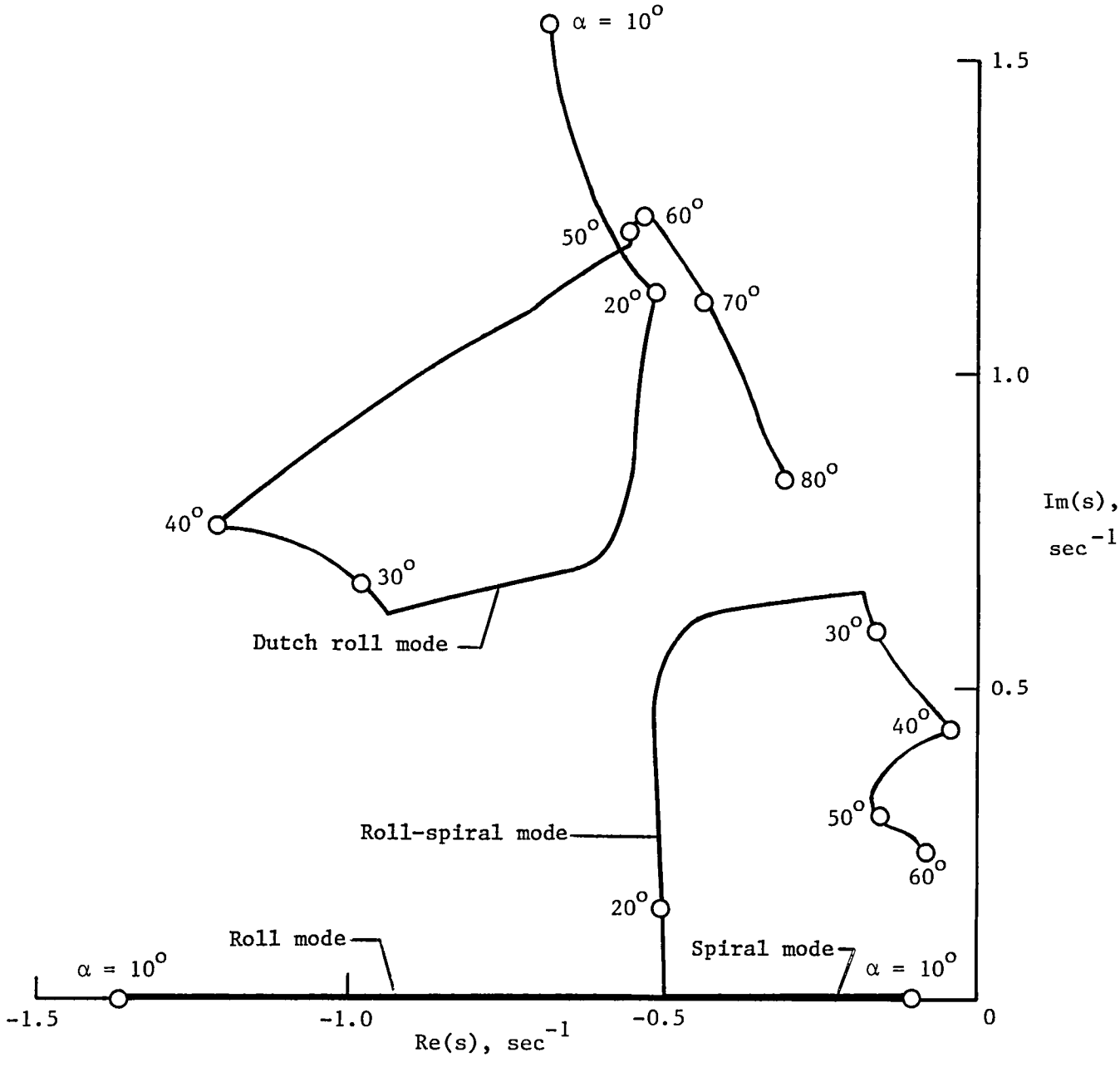

Figure 9. Lateral open-loop poles as functions of angle of attack.

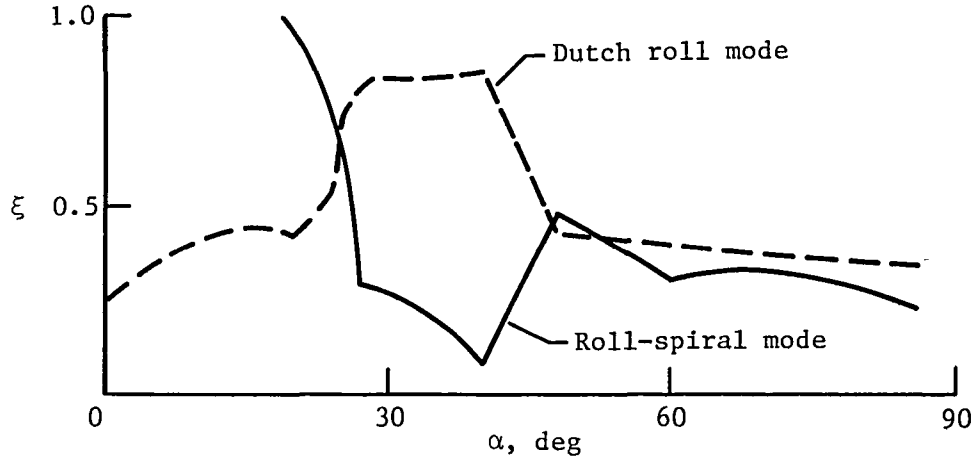

(a) Damping.

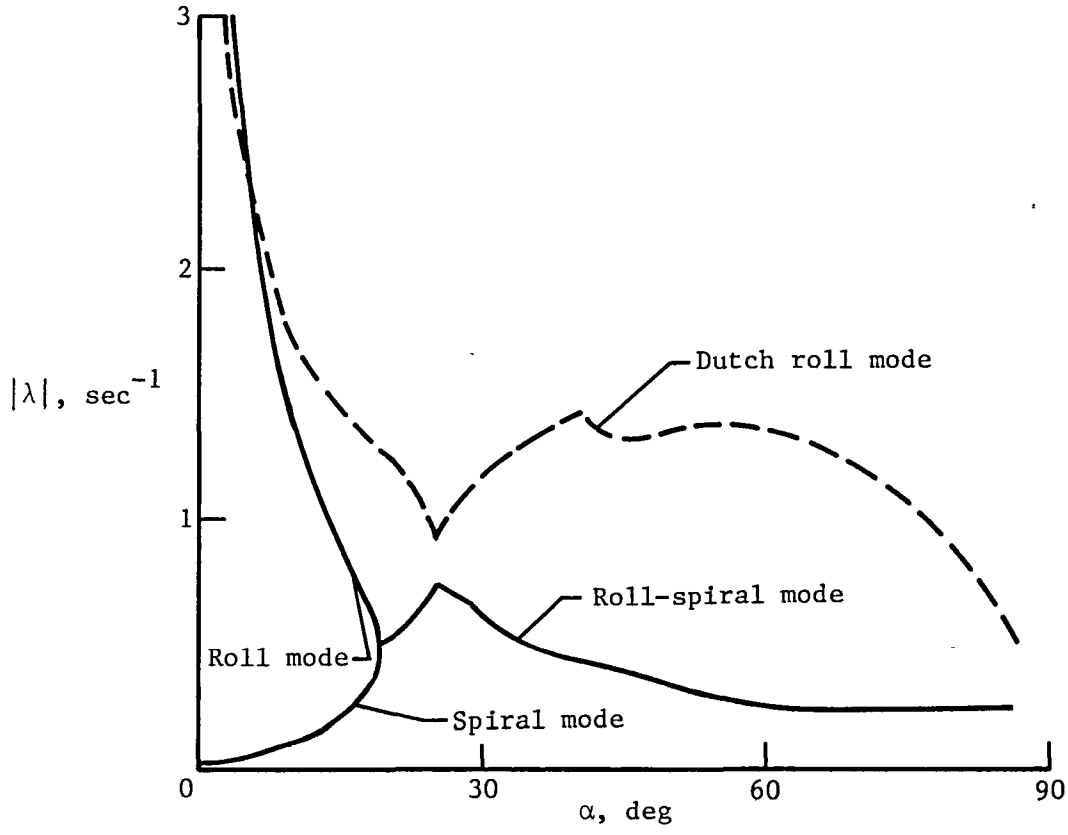

(b) Frequency.

Figure 10 Frequency and damping of lateral-directional modes.

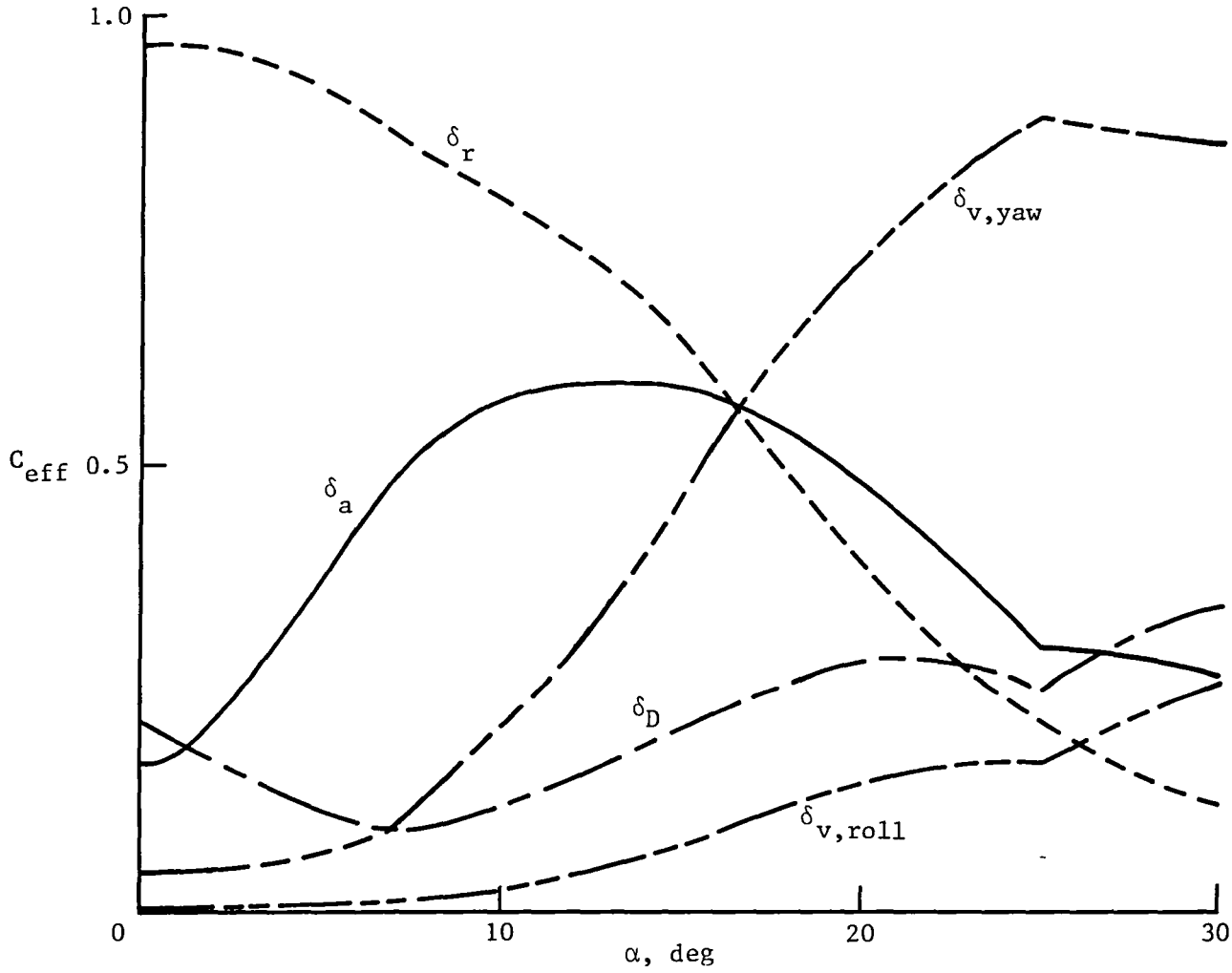

Figure 11. Relative effectiveness of lateral controls on Dutch roll mode.

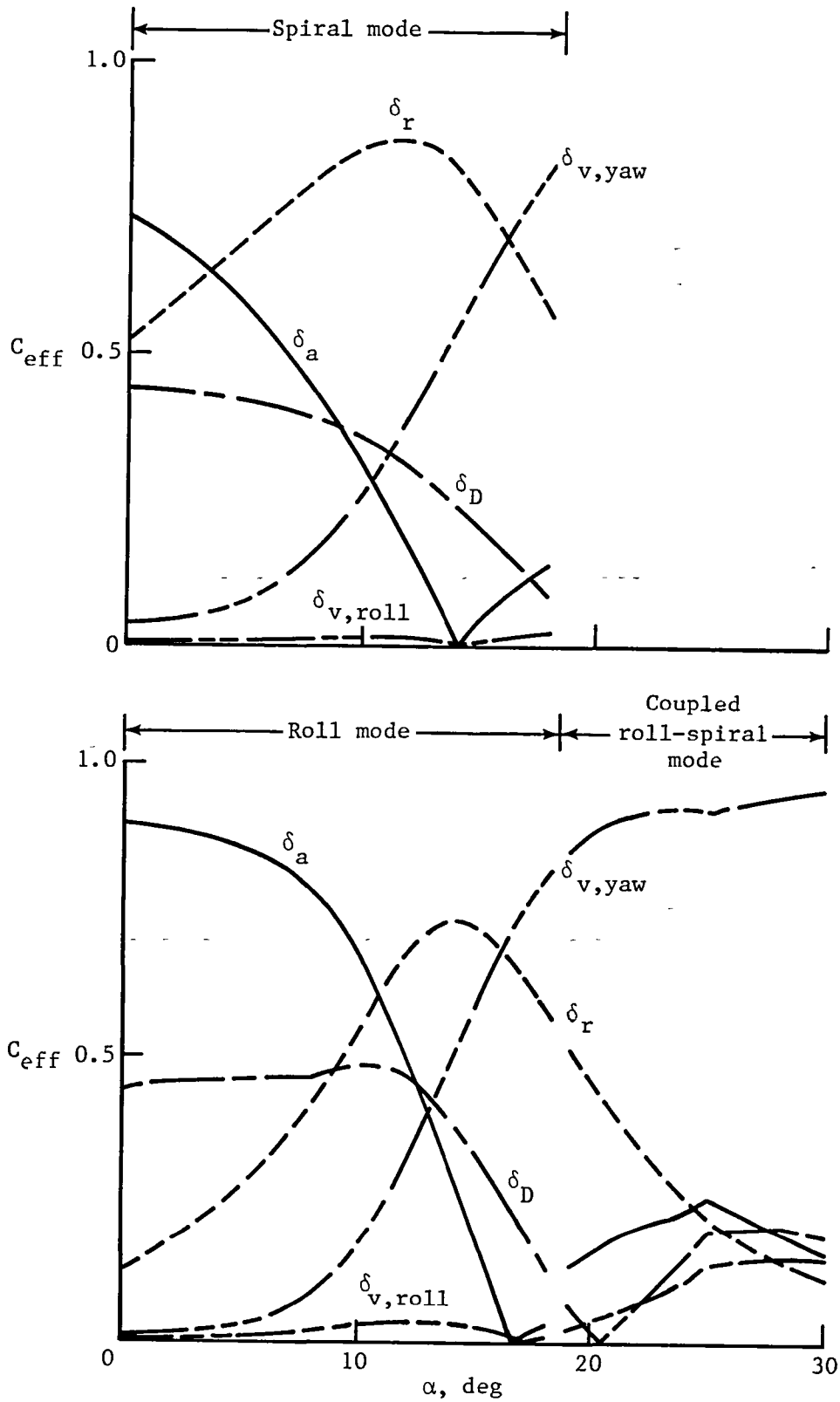

Figure 12. Relative effectiveness of lateral controls on roll and spiral modes.

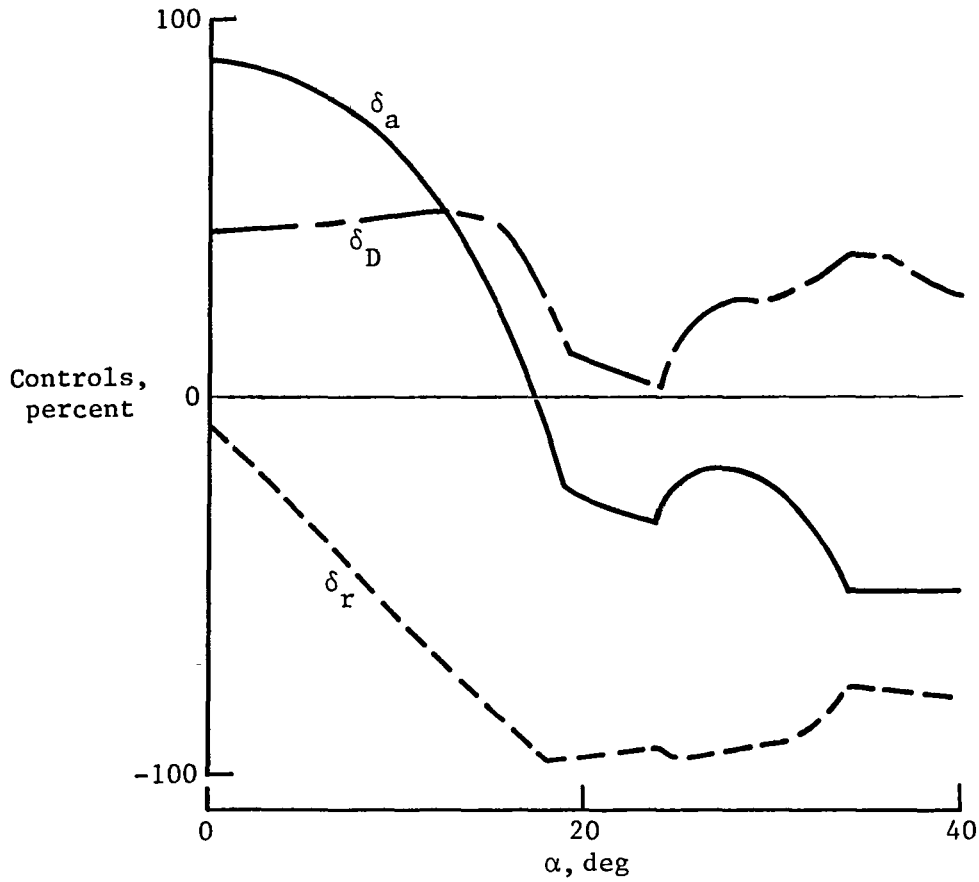

Figure 13 Aerodynamic control interconnects for lateral control.

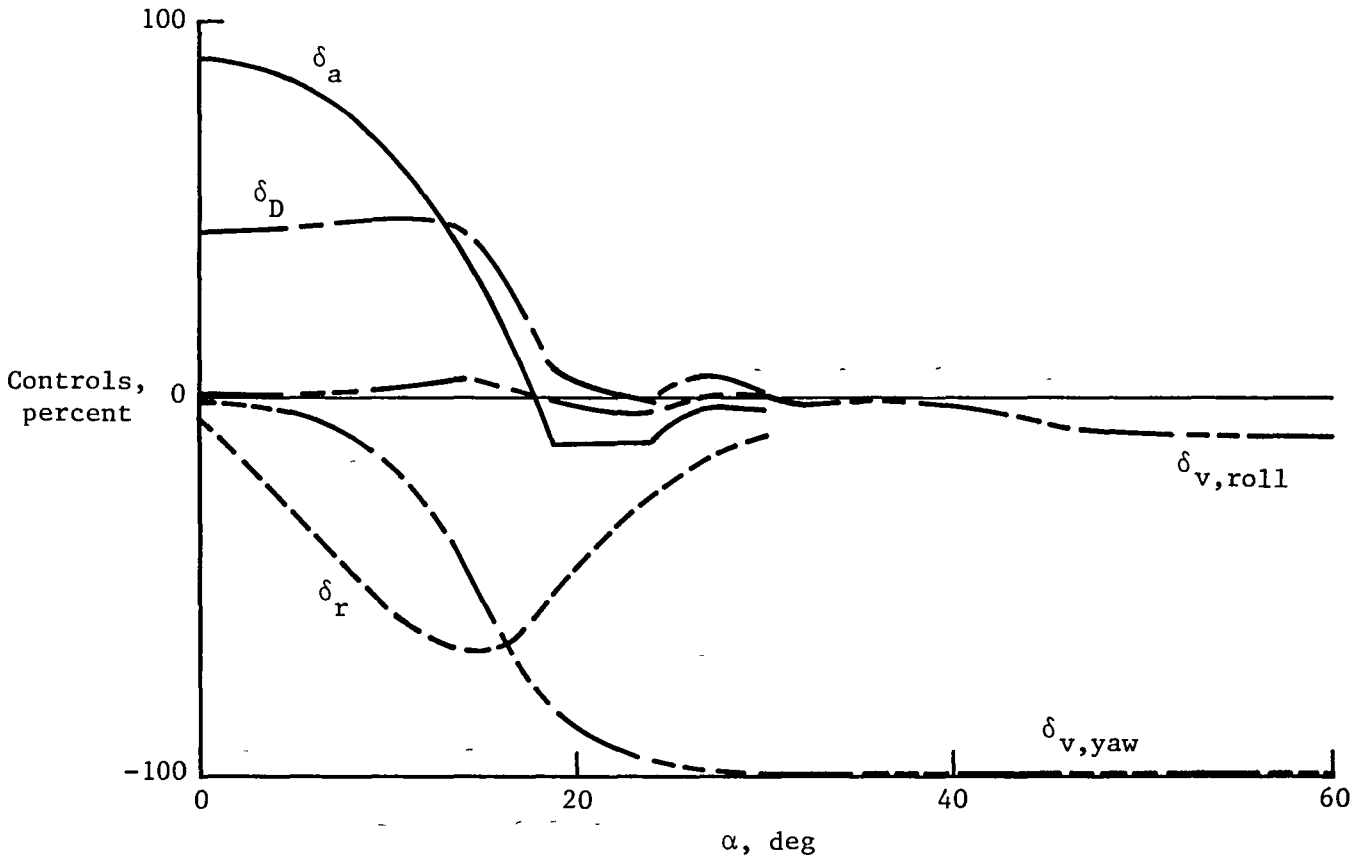

Figure 14. Control interconnects for lateral control.

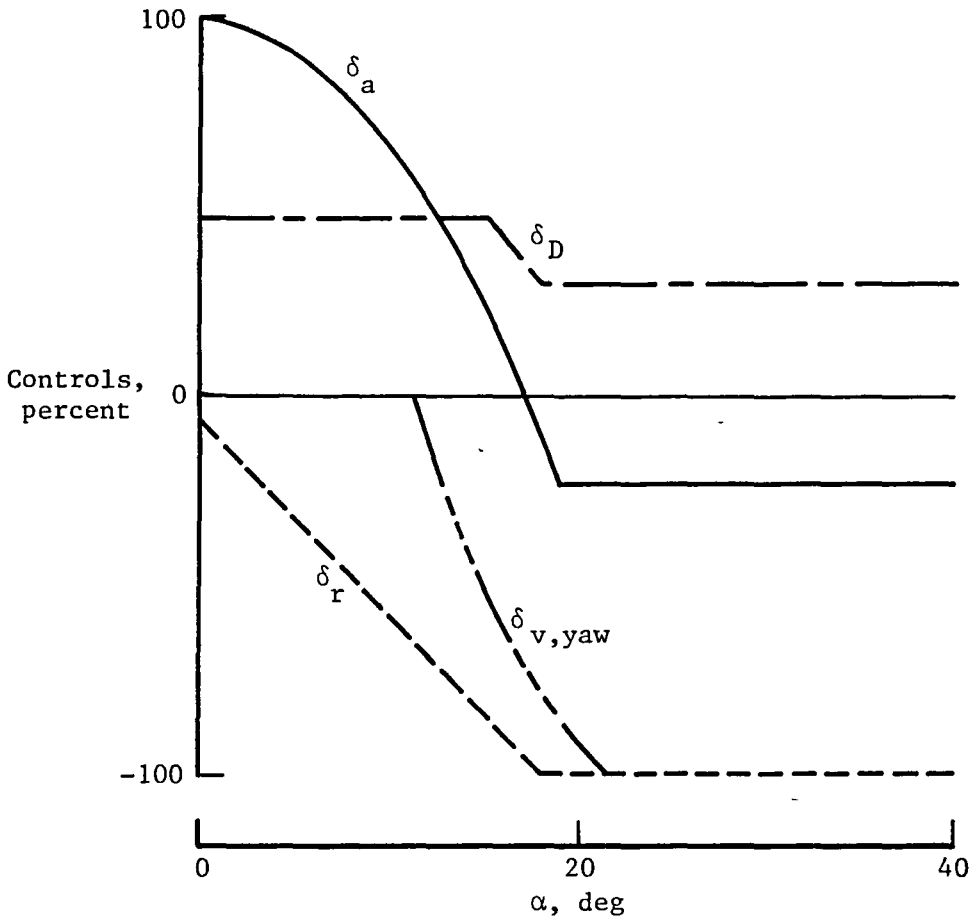

Figure 15. Interconnect schedules for lateral pseudo control, v_{lat}.

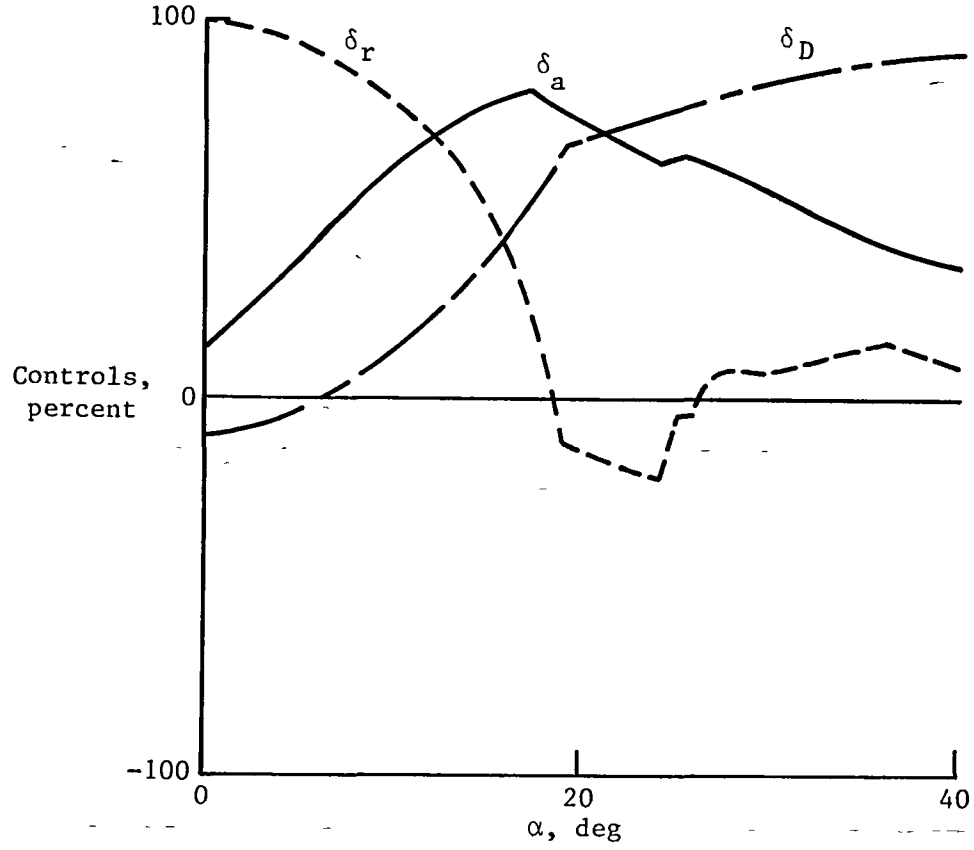

Figure 16. Aerodynamic control interconnects for directional control.

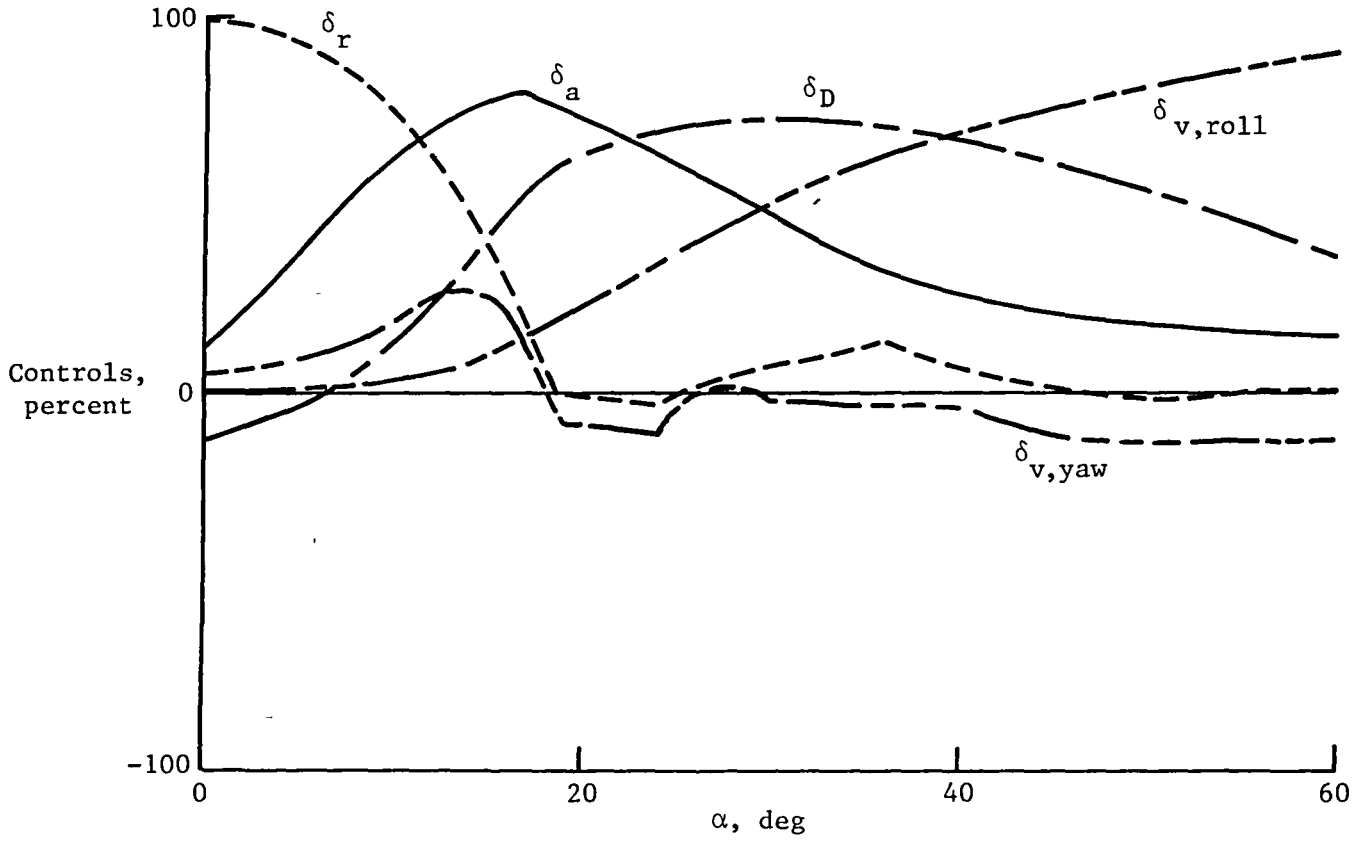

Figure 17. Control interconnects for directional control.

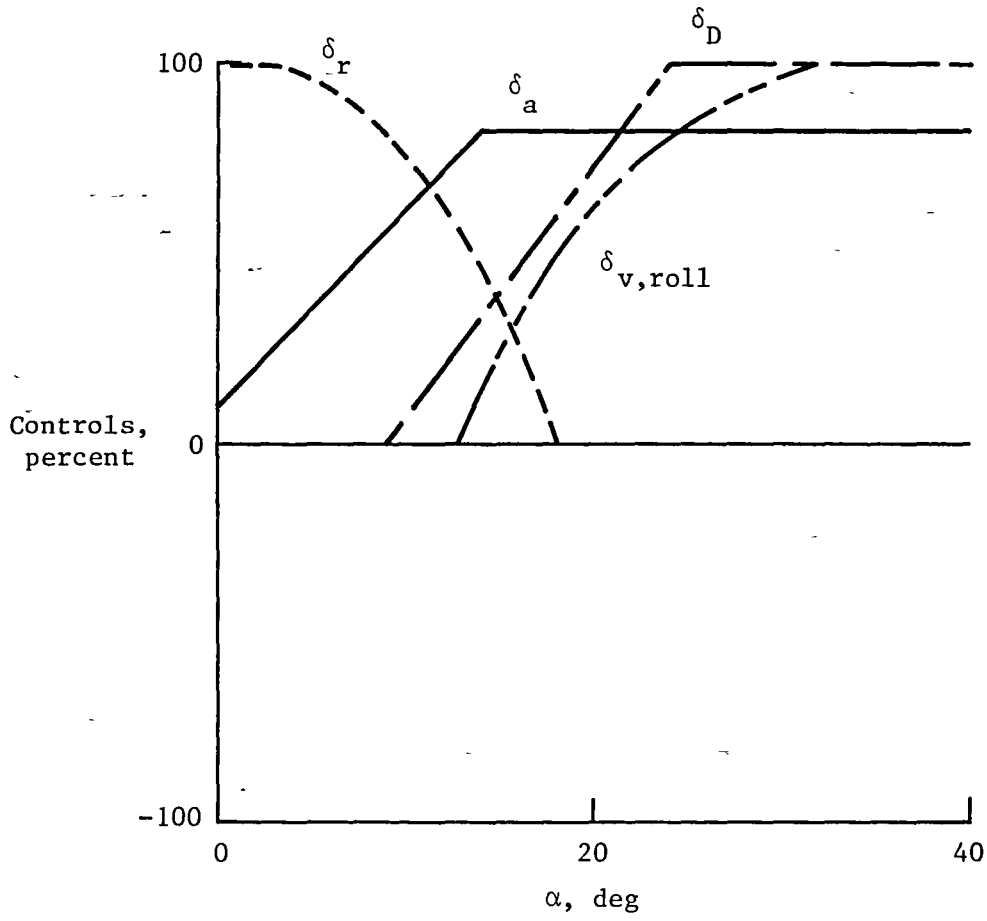

Figure 18. Interconnect schedules for directional pseudo control, v_{dir}.

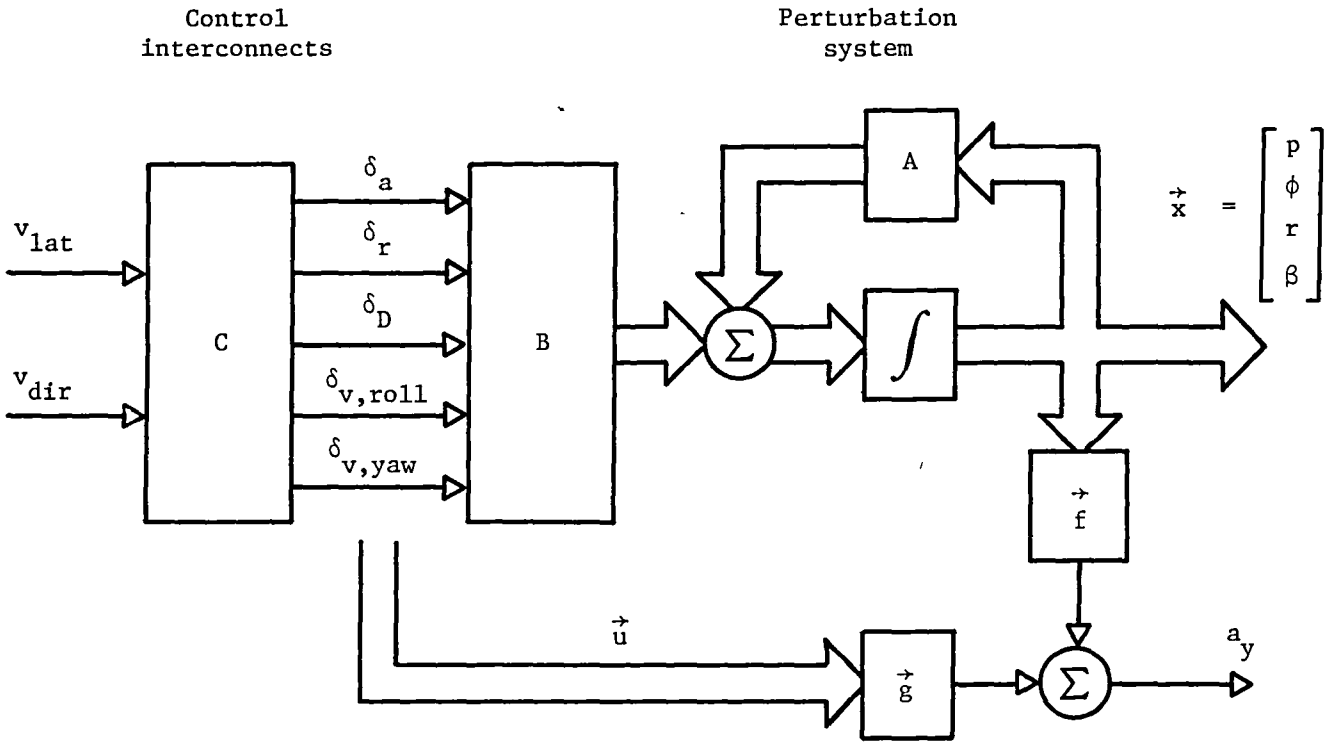

Figure 19 Modified perturbation system.

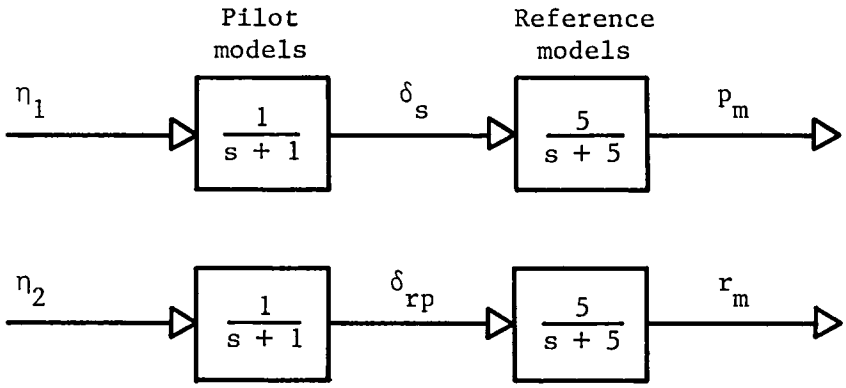

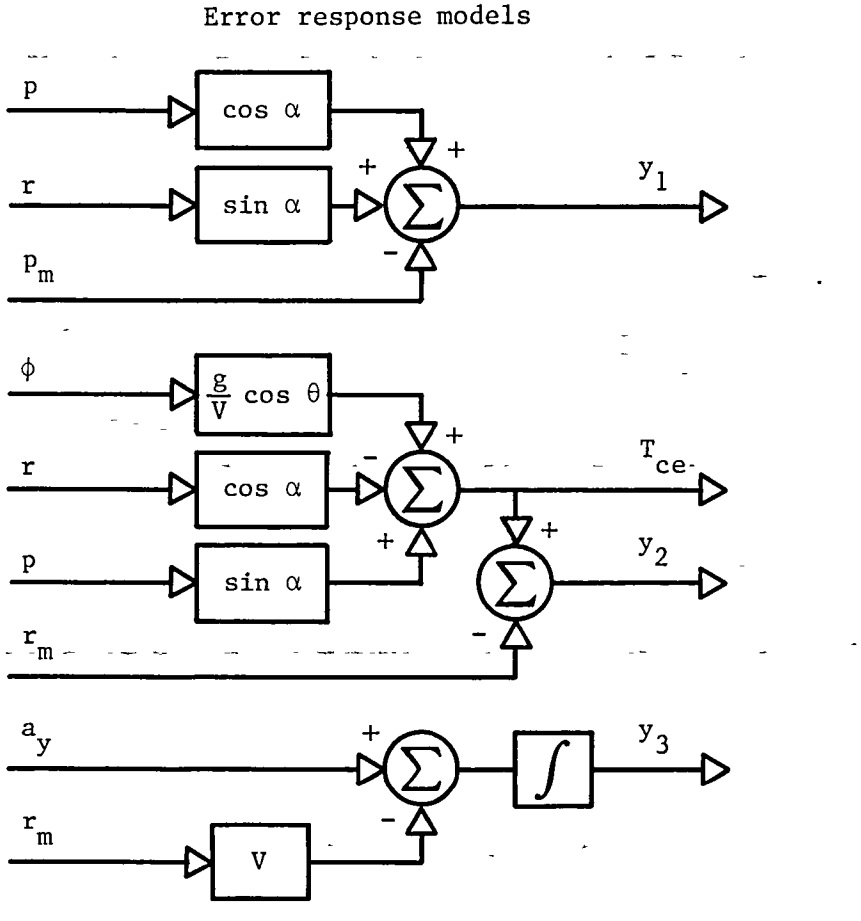

Figure 20. Auxiliary models.

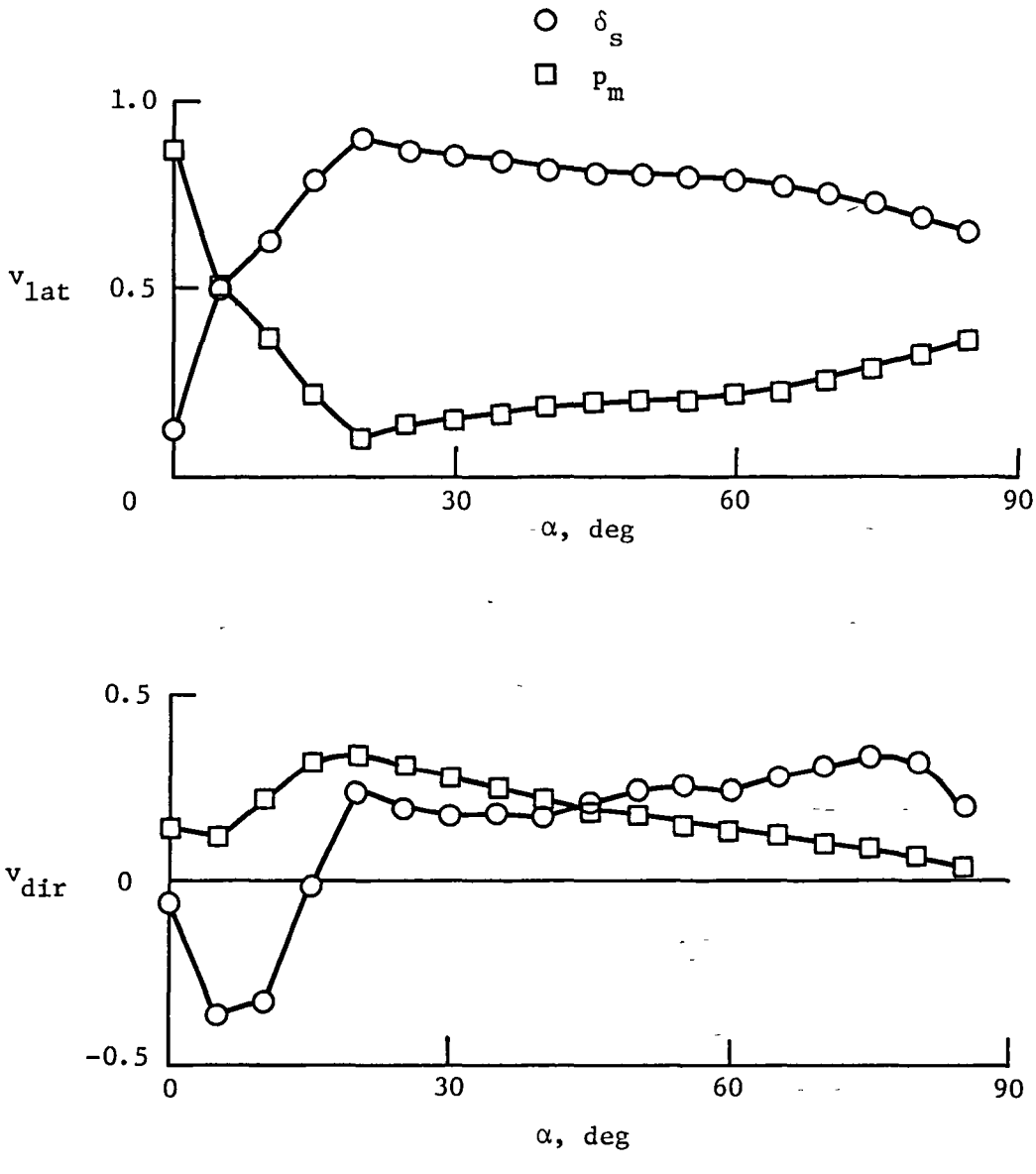

(a) Lateral stick and roll rate model.

Figure 21. Measurement vector gains

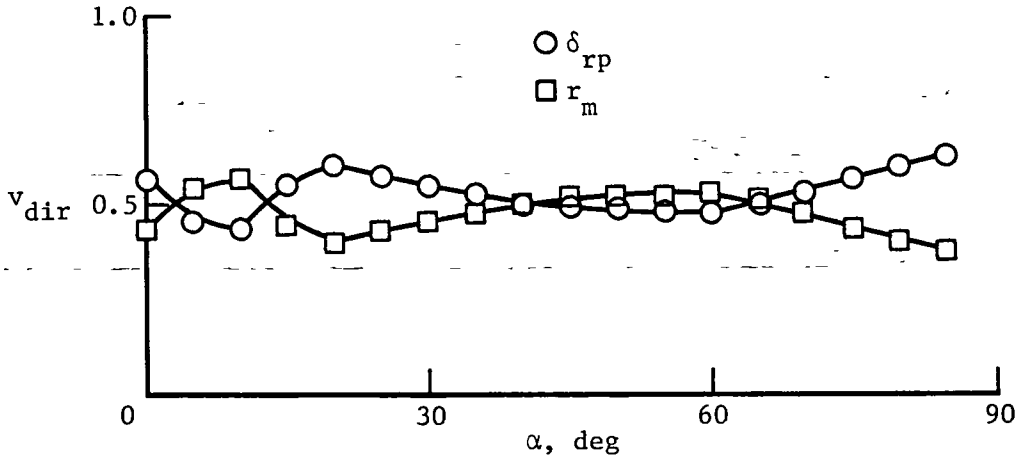

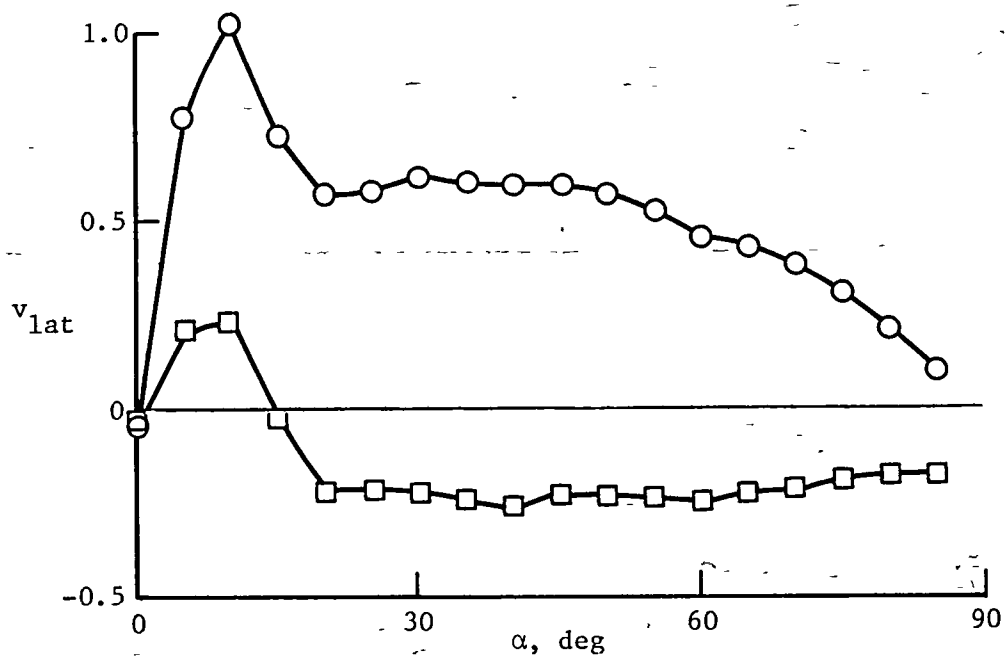

(b) Rudder pedals and yaw rate model.

Figure 21. Continued.

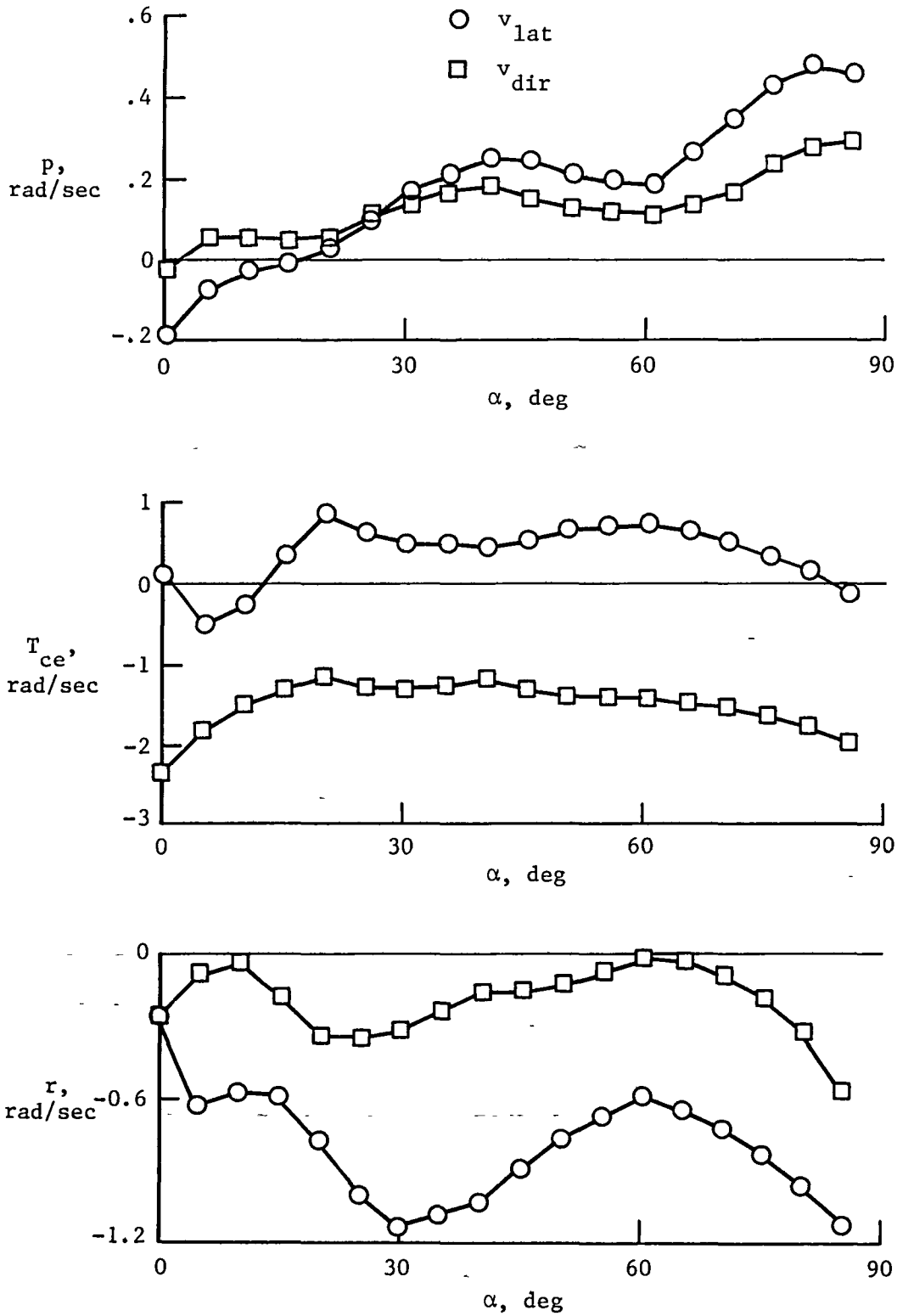

(c) Body-axis rates and turn coordination error.

Figure 21. Continued.

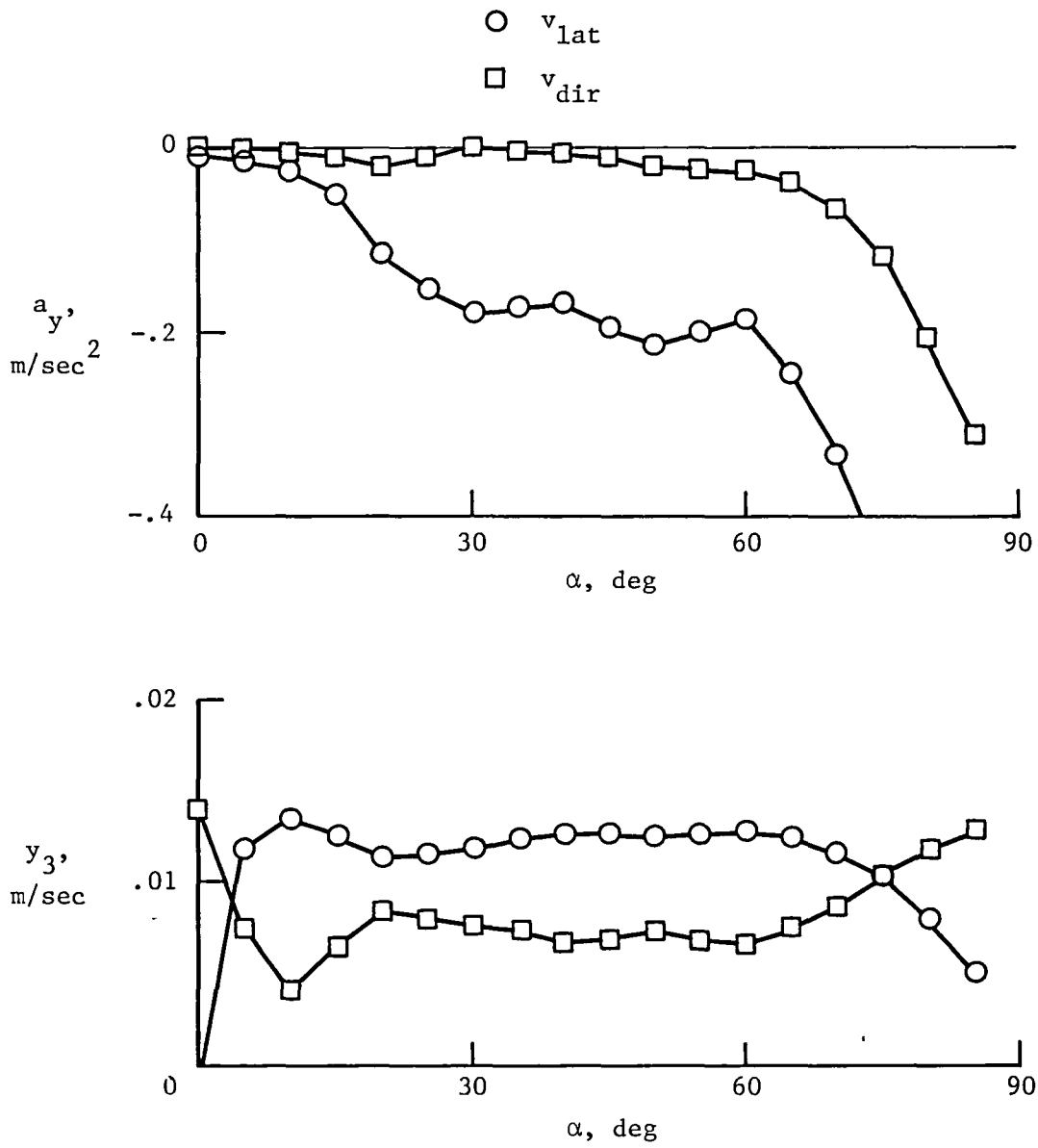

(d) Lateral acceleration.

Figure 21 Concluded

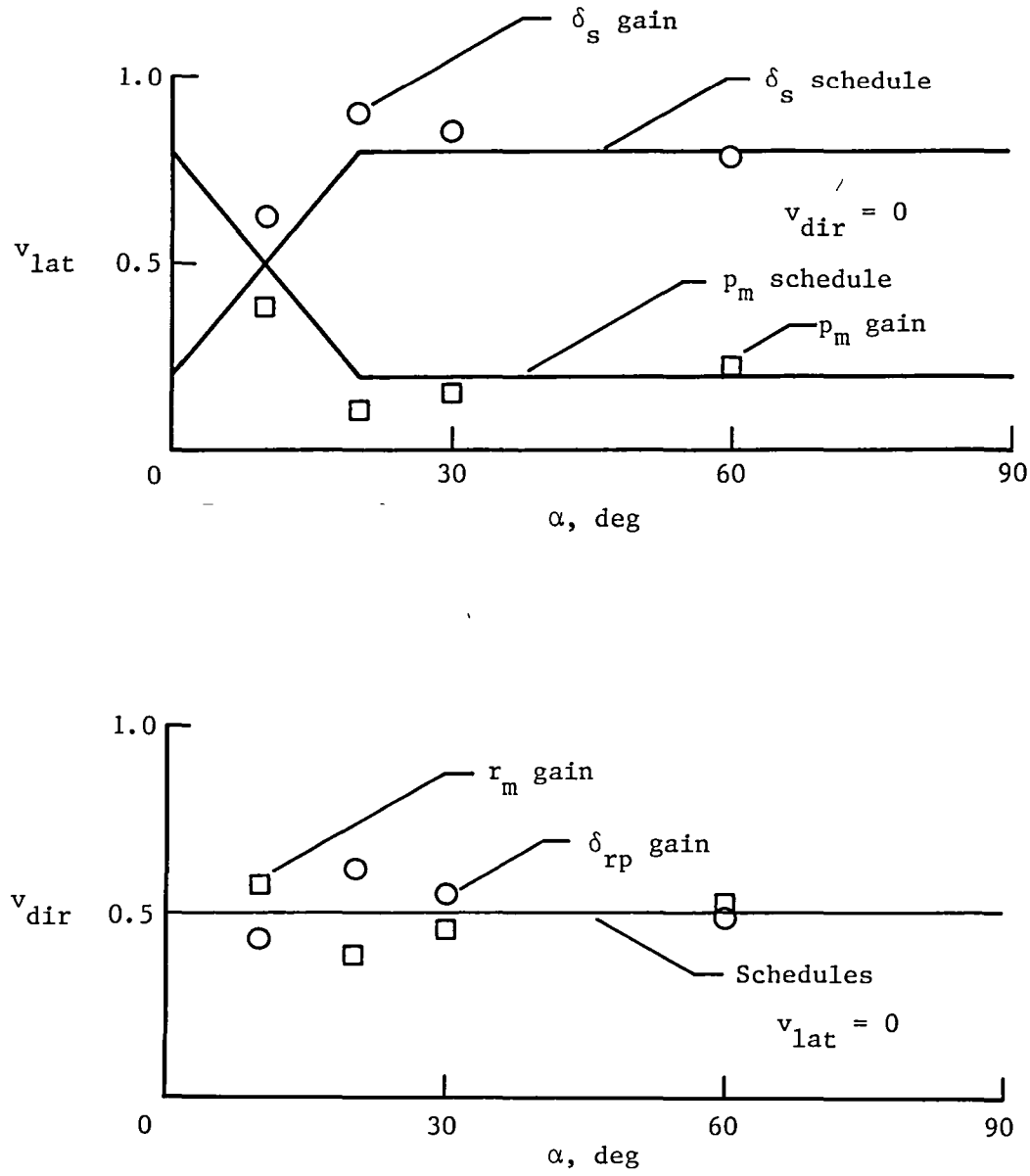

(a) Pilot controls and rate models.

Figure 22. Gain schedules.

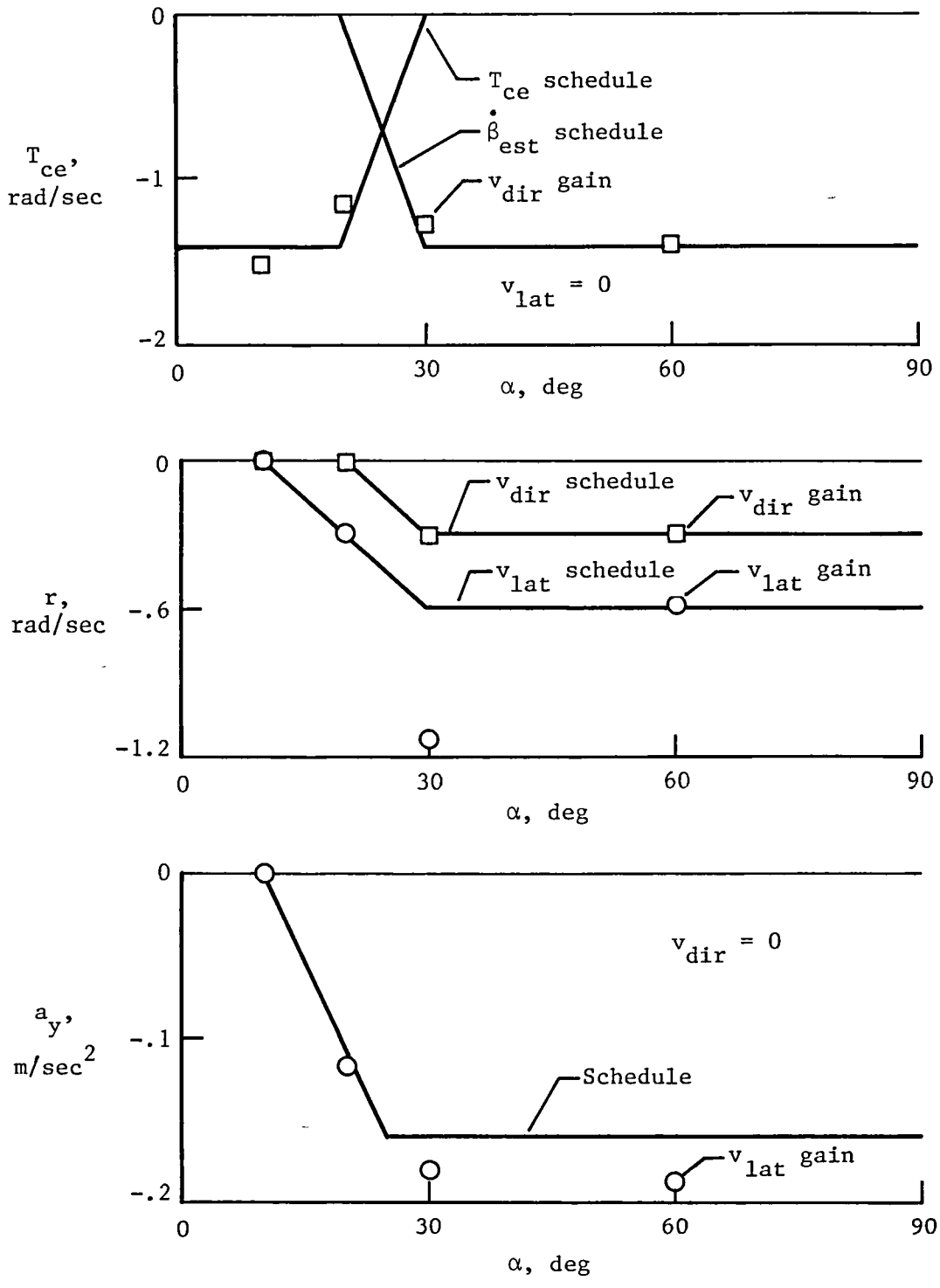

(b) Airplane motion feedback gains.

Figure 22. Concluded.

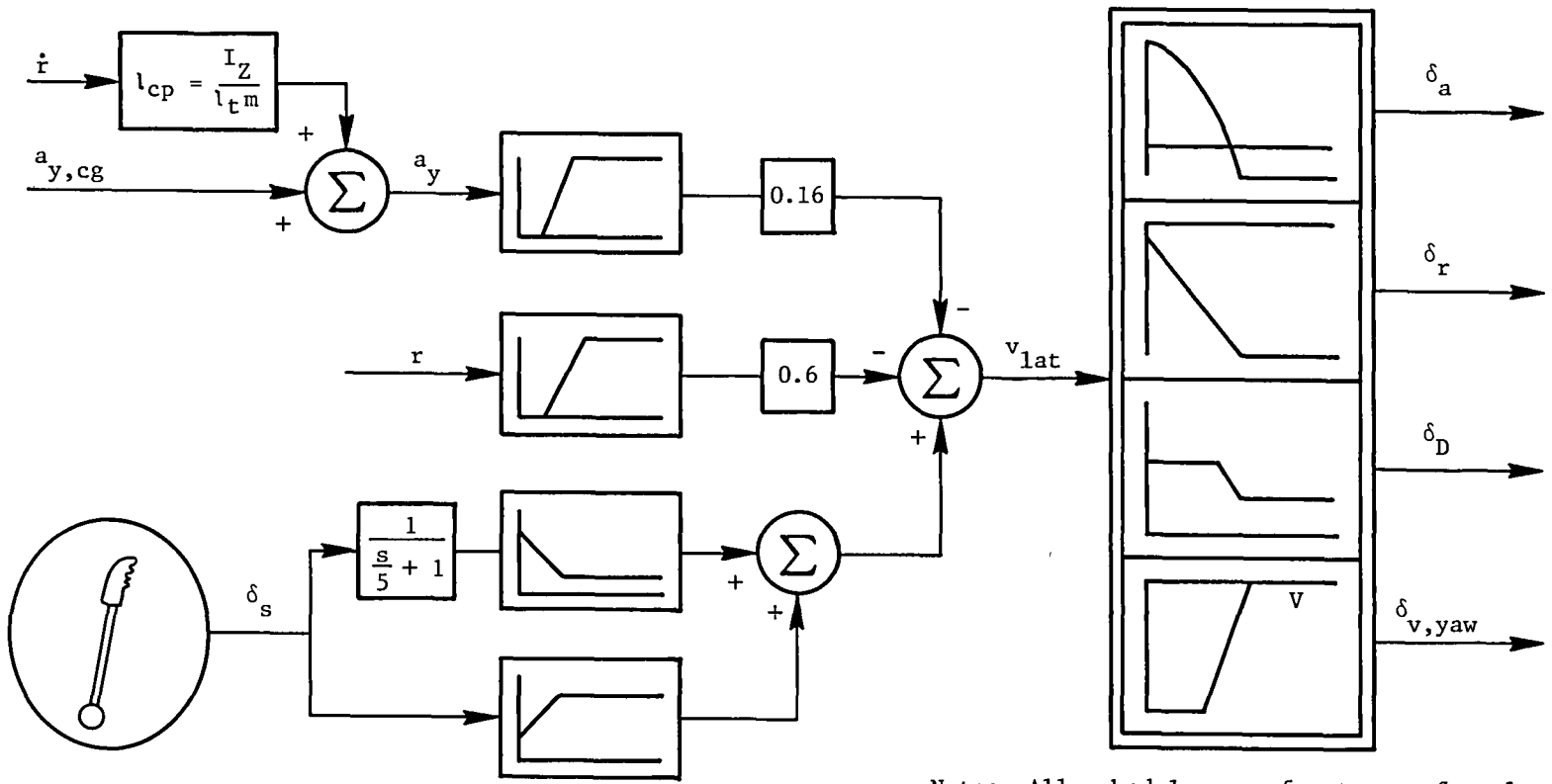

(a) Lateral channel.

Figure 23. Control systems.

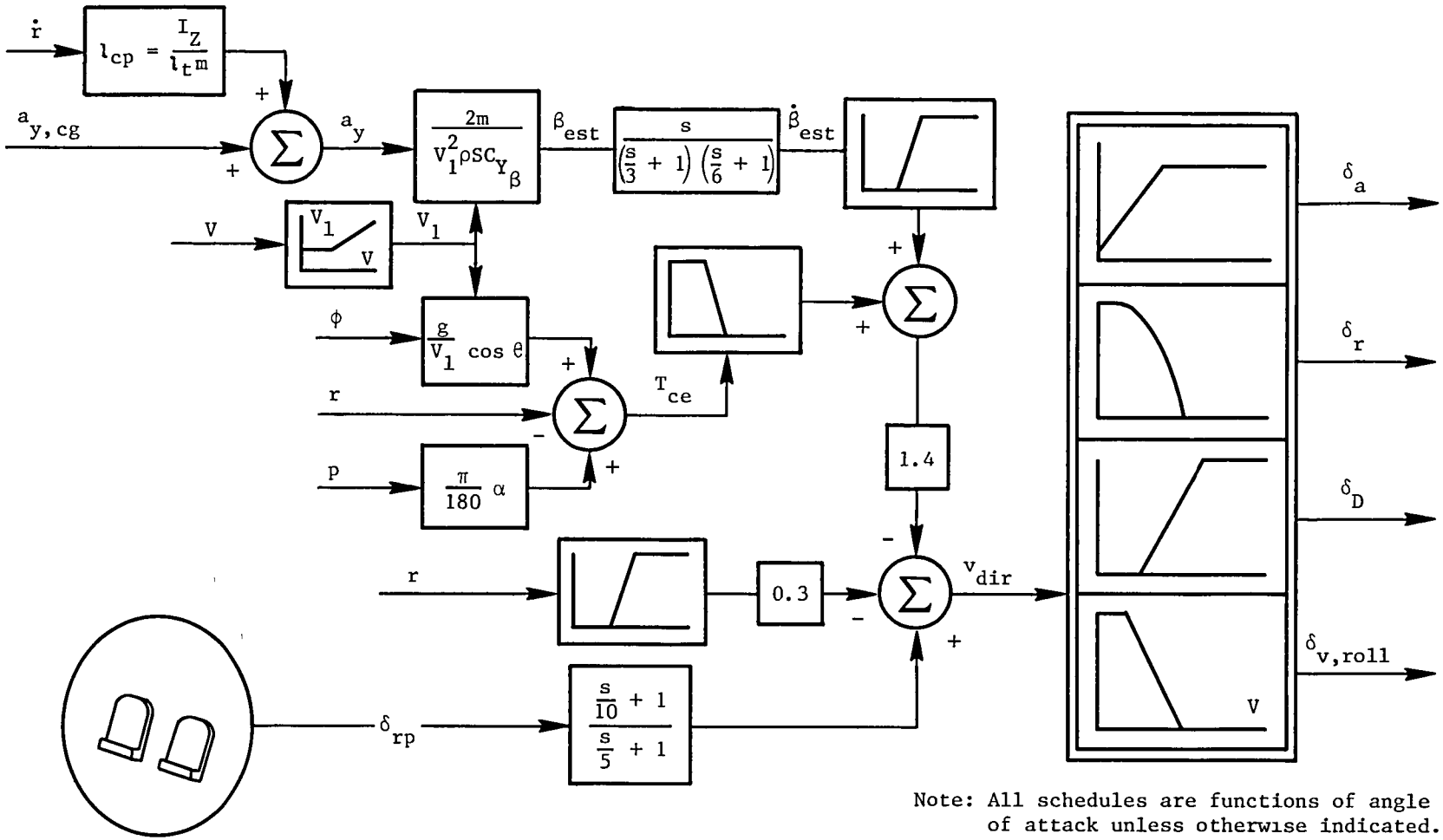

Note: All schedules are functions of angle of attack unless otherwise indicated.

(b) Directional channel.

Figure 23. Concluded.

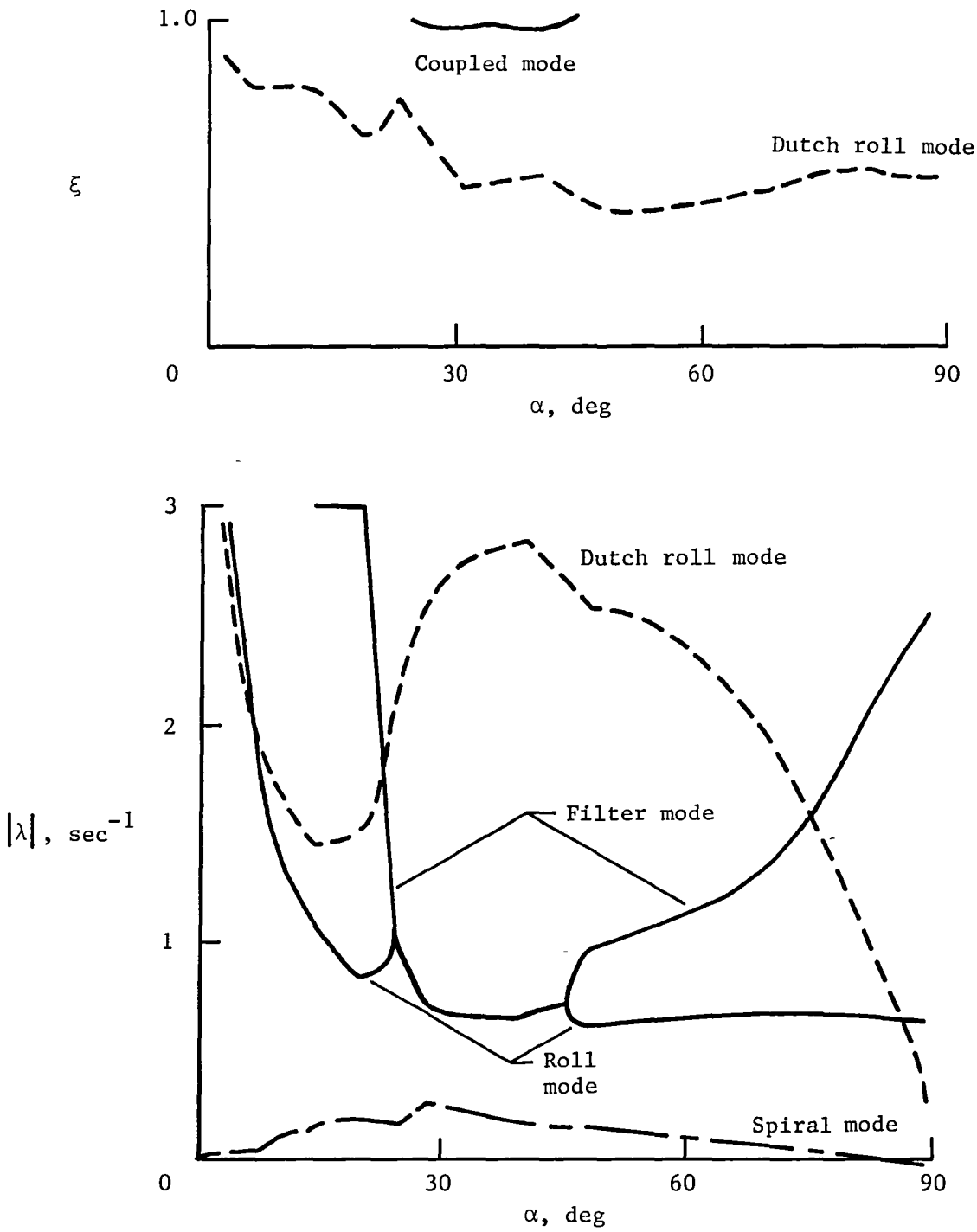

Figure 24. Frequency and damping of closed-loop modes

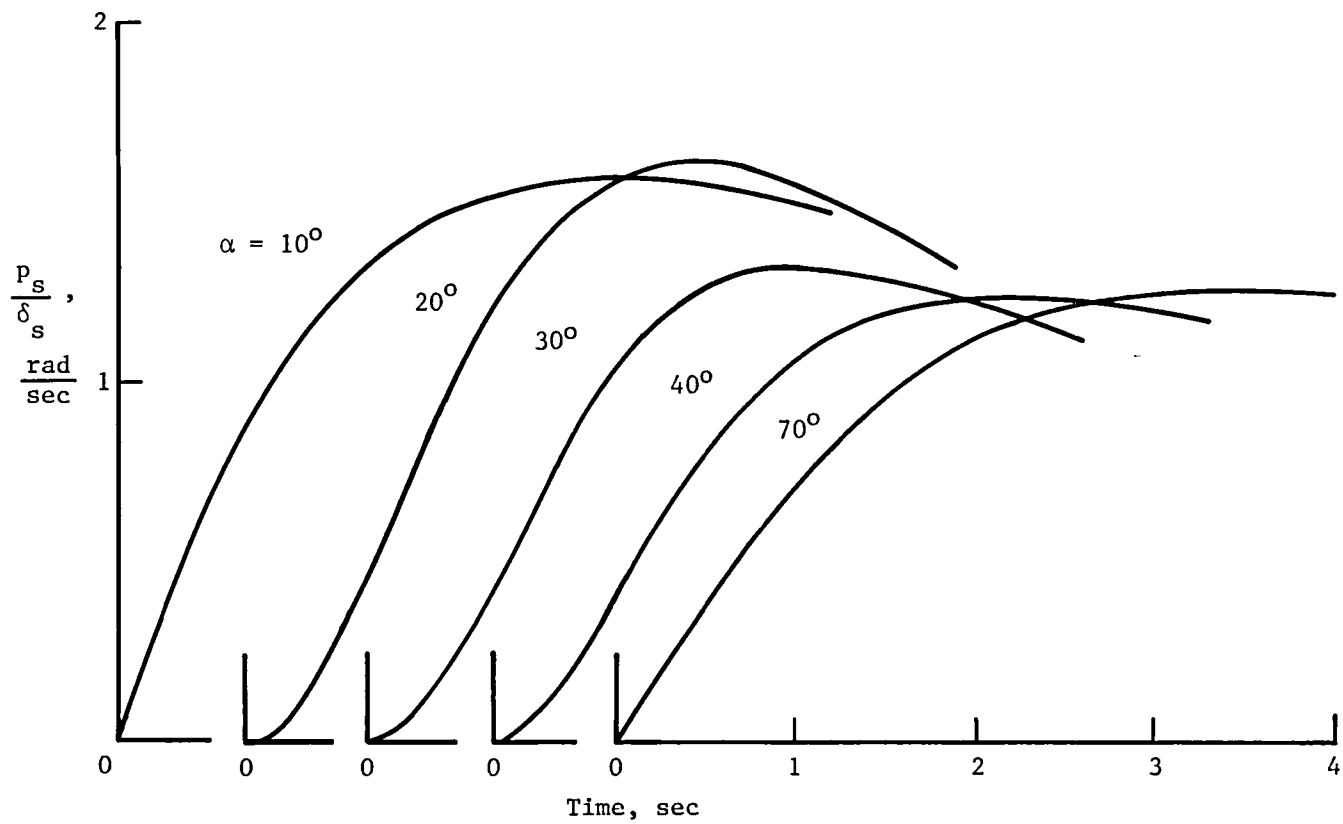

(a) Normalized stability axis roll rate response to lateral stick step input.

Figure 25. Airplane responses to pilot controls.

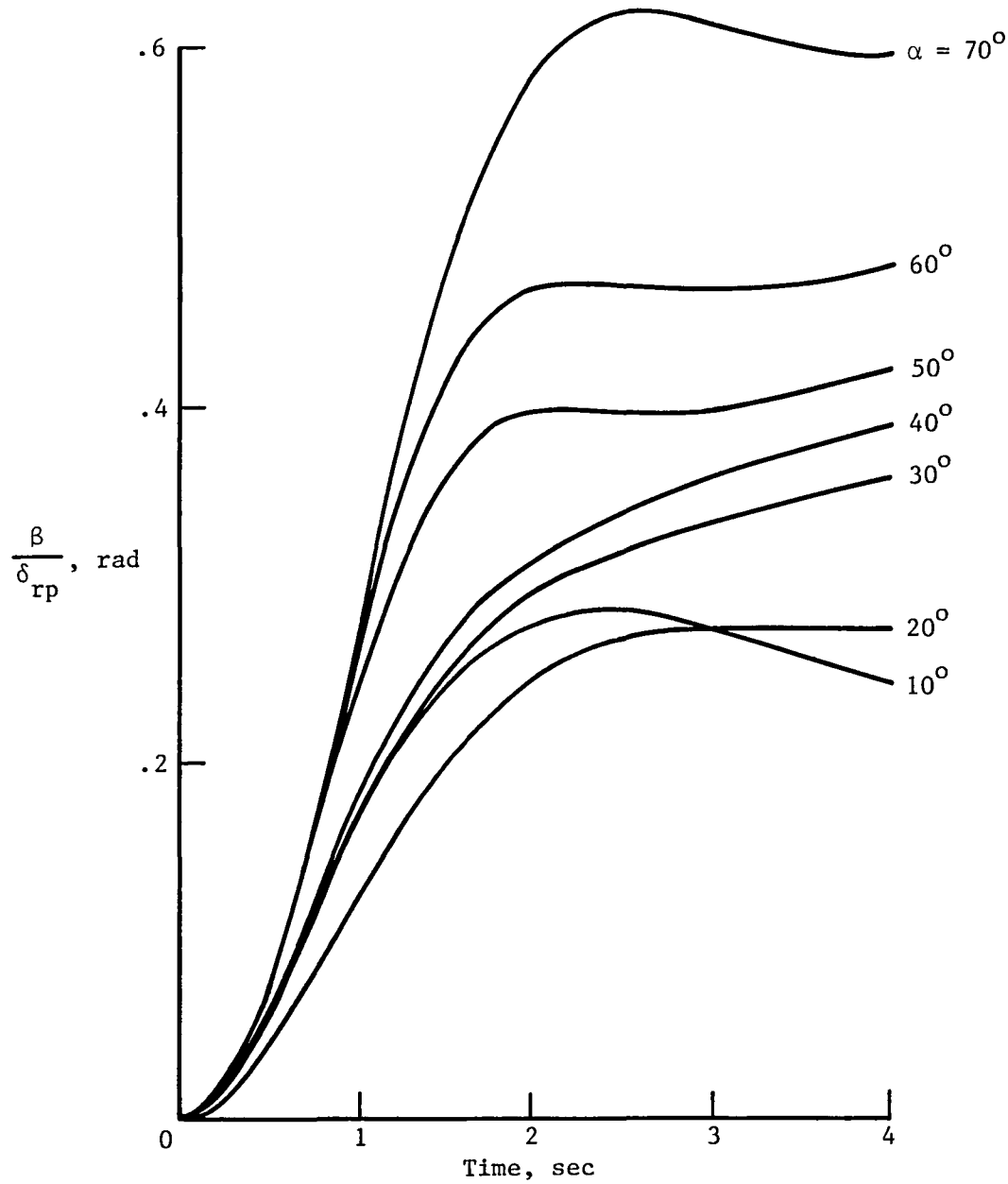

(b) Normalized sideslip responses to rudder pedal.

Figure 25. Concluded.

1 Report No	2 Government Accession No	3 Recipient's Catalog No
NASA TM-86425		

4 Title and Subtitle	5 Report Date
Preliminary Design Study of a Lateral-Directional Control System Using Thrust Vectoring	November 1985
	6 Performing Organization Code: 505-34-03-02
7 Author(s): Frederick J Lallman	8 Performing Organization Report No: L-15990
9 Performing Organization Name and Address: NASA Langley Research Center, Hampton, VA 23665-5225	10 Work Unit No
	11 Contract or Grant No
12 Sponsoring Agency Name and Address: National Aeronautics and Space Administration, Washington, DC 20546-0001	13 Type of Report and Period Covered: Technical Memorandum
	14 Sponsoring Agency Code

15 Supplementary Notes

16 Abstract

A preliminary design of a lateral-directional control system for a fighter airplane capable of controlled operation at extreme angles of attack is developed. The subject airplane is representative of a modern twin-engine high-performance jet fighter. It is equipped with ailerons, rudder, and independent horizontal-tail surfaces. Idealized bidirectional thrust-vectoring engine nozzles are appended to the mathematic model of the airplane to provide additional control moments Optimal schedules for lateral and directional pseudo control variables are calculated. Use of pseudo controls results in coordinated operation of the aerodynamic and thrust-vectoring controls with minimum coupling between the lateral and directional airplane dynamics. Linear quadratic regulator designs are then used to specify a preliminary flight control system to improve the stability and response characteristics of the airplane Simulated responses to step pilot control inputs are stable and well behaved. For lateral stick deflections, peak stability axis roll rates are between 1.25 and 1 60 rad/sec over an angle-of-attack range of 10° to 70°. For rudder pedal deflections, the roll rates accompanying the sideslip responses can be arrested by small lateral stick motions.

17 Key Words (Suggested by Authors(s))	18 Distribution Statement
Airplane control Integrated control Thrust-vectoring control Optimization Controllability	Unclassified—Unlimited Subject Category 08

19 Security Classif (of this report)	20 Security Classif (of this page)	21 No of Pages	22 Price
Unclassified	Unclassified	49	A03

For sale by the National Technical Information Service, Springfield, Virginia 22161

NASA-Langley, 1985

End of Document